Inorg. Chem. **2008**, *47*, 8000−8015

Enantiopure, Supramolecular Helices Containing Three-Dimensional Tetranuclear Lanthanide(III) Arrays: Synthesis, Structure, Properties, and Solvent-Driven Trinuclear/Tetranuclear Interconversion

Marco Lama,[†] Olimpia Mamula,[*,†,⊥] Gregg S. Kottas,[‡] Luisa De Cola,[‡] Helen Stoeckli-Evans,[§] and Sergiu Shova[||]

Institut des sciences et ingénierie chimiques, Ecole Polytechnique Fédérale de Lausanne, BCH 1403, 1015 Lausanne, Switzerland, Physikalisches Institut, Westfälische Wilhelms-Universität Münster, Mendelstrasse 7, D-48149 Münster, Germany, Institut de microtechnologie, Université de Neuchâtel, Rue Emile-Argand 11, 2009 Neuchâtel, Switzerland, and Department of Chemistry, Moldova State University, A. Mateevici 60, 2009 Chisinau, Moldova

Received October 24, 2007

The enantiomerically pure pinene-bipyridine-based receptor, (−) or (+) L^-, diastereoselectively self-assembles in dry acetonitrile in the presence of Ln^{III} ions (Ln = La, Pr, Nd, Sm, Eu, Gd, and Tb) to give a C_3-symmetrical, pyramidal architecture with the general formula $[Ln_4(L)_9(\mu_3\text{-}OH)](ClO_4)_2$ (abbreviated as *tetra*-Ln_4L_9). Three metal centers shape the base: an equilateral triangle surrounded by two sets of helically wrapping ligands with opposite configurations. This part of the structure is very similar to the species $[Ln_3(L)_6(\mu_3\text{-}OH)(H_2O)_3](ClO_4)_2$ (recently reported by us and abbreviated as *tris*-LnL_2) formed by the ligand and the Ln(III) ions when the reactions are performed in methanol. The tetranuclear structure is completed by a capping, helical unit LnL_3 whose chirality is also predetermined by the chirality of the ligand. A complete characterization of these isostructural, chiral compounds was performed in solid state (X-ray, IR) and in solution (ES-MS, NMR, CD, UV−vis and emission spectroscopies). The sign and the intensity of the CD bands in the region of the $\pi\pi^*$ transitions of the bipyridine (absolute $\Delta\varepsilon$ values at 327 nm are about 280 $M^{-1}\cdot cm^{-1}$) are highly influenced by the helicity of the capping fragment LnL_3. The photophysical properties (lifetime, quantum yield) of the visible (Eu and Tb complexes) and NIR (Nd complex) emitters indicate a good energy transfer between the ligands and the metal centers. The two related superstructures *tetra*-Ln_4L_9 and *tris*-LnL_2 can be interconverted in acetonitrile, the switching process depending on the amount of water present in the solvent, the size of the Ln(III) ion, and the concentration. The weak chiral recognition capabilities of the self-assembly leading to the formation of *tetra*-Ln_4L_9 either by direct synthesis from a racemic mixture of the ligand and Ln(III) ions or by the conversion of a *tris*-$Ln[(\pm)\text{-}L]_2$ racemate were likewise demonstrated.

Introduction

Because of their electronic structure, with partially filled 4f orbitals shielded from external perturbations by outer 5s and 5p orbitals, the lanthanide (Ln) ions possess very interesting chemical, magnetic, and photophysical properties.[1–4] Their incorporation into self-assembled, supramolecular entities is thus very promising in view of obtaining new, improved catalysts, luminescent sensors, and materials.[5–8] In contrast with the d-metal ions, the Ln ions are

* To whom correspondence should be addressed. E-mail:olimpia.mamula.steiner@gmail.com. Fax: (+41) 21-693-9815.
[†] Ecole Polytechnique Fédérale de Lausanne.
[‡] Westfälische Wilhelms-Universität Münster.
[§] Université de Neuchâtel.
[||] Moldova State University.
[⊥] Present address: Swatch Group R&D Ltd., Rve de Sors 3, CH-2074 Marin, Switzerland.

(1) Choppin, G. R. In *Lanthanide Probes in Life, Chemical and Earth Sciences*; Bünzli, J-C. G. , Choppin, G. R. Eds.; Elsevier: Amsterdam, 1989.
(2) Mikami, K.; Terada, M.; Matsuzawa, H. *Angew. Chem., Int. Ed.* **2002**, *41*, 3554.
(3) Parker, D.; Dickins, R. S.; Puschmann, H.; Crossland, C.; Howard, J. A. K. *Chem. Rev.* **2002**, *102*, 1977.
(4) Selvin, P. R. *Annu. Rev. Biophys. Biomol. Struct.* **2002**, *31*, 275.
(5) Faulkner, S.; Mathews, J. L. *Comprehensive coordination chemistry*, 2nd ed.; Elsevier,: Amsterdam, 2003; Vol. *9*.
(6) Parker, D. *Chem. Soc. Rev.* **2004**, *33*, 156.
(7) Parker, D.; Williams, J. A. G. *Metal ions in biological systems: The Lanthanides and Their Interrelations with Biosystems*; A. Sigel, H. Sigel Eds.; Marcel Dekker: New York, 2003; Vol. *40*, pp 233−280.
(8) McCoy, C. P.; Stomeo, F.; Plush, S. E.; Gunnlaugsson, T. *Chem. Mater.* **2006**, *18*, 4336.

10.1021/ic7021006 CCC: $40.75
Published on Web 08/12/2008

characterized by high and versatile coordination numbers as well as weak stereochemical preferences. These are strong drawbacks in the synthesis of structurally well defined lanthanide arrays; indeed, in the Ln series, there are only few examples of nonpolymeric, coordination compounds containing three or more metal centers.[9–11] On the other hand, there are many high nuclearity compounds based on d-metal ions, their structures being easier to control and to predict. Moreover, some of these structures showing a supramolecular helical chirality type, the helicates, have been isolated in their enantiopure form either by resolution of a racemate or by diastereoselective synthesis.[12,13] In the case of lanthanide complexes with nuclearity equal to three or higher, in addition to our work,[14–16] only one other example, that of the diastereoselective synthesis of a remarkable enantiopure chiral nanoball containing 18 lanthanum ions, has been reported recently.[17]

Previously, we have shown that the reaction *in methanol* between a pinene bipyridine carboxylic ligand HL (see Scheme 1, left) and almost all the Ln ions of the series leads to the diastereoselective formation of an enantiopure supramolecular helical architecture containing three metal centers disposed in the corners of an equilateral triangle.

Six ligands forming two helical domains with opposite orientations wrap around this metal core ensuring, together with a hydroxide group situated on the C_3 axis, the cohesion of the structure.[14] The synthesis, as well as the thoroughly investigated properties of this class of compounds, has been recently described.[16] Furthermore, we have demonstrated that in the case of Pr(III) ions the reaction *in anhydrous acetonitrile* does not lead to the formation of the trinuclear structure as was the case in methanol. In this case a tetranuclear structure with the formula $[Pr_4L_9(OH)](ClO_4)_2$ was quantitatively obtained (Scheme 1, right). Interestingly, the trinuclear and the tetranuclear compounds can be reversibly interconverted in acetonitrile simply by varying the amount of water present in the solvent.[15] This is an unique and remarkable example in the Ln series of "constitutional dynamic chemistry".[18–20] This concept, developed for structures containing d-metal ions (with the exception of one example in the f series[21]), concerns the capacity of a metallo-supramolecular architecture to adapt its structure to various changes of external stimuli, especially the concentration[22–25] or the presence of a template agent.[26–33] The solvent is another important factor able to control the equilibrium ratio, and few examples of solvent-dependent interconverting systems containing d-metal ions have been reported as well.[34–43]

This paper describes, in the first part, the synthesis and the properties of the tetranuclear class of lanthanide arrays with the general formula $[Ln_4L_9(\mu_3\text{-}OH)](ClO_4)_2$, abbreviated in the text as *tetra*-Ln_4L_9. The second part presents the detailed studies of the factors influencing the reversible switching between the trinuclear architecture $[Ln_3L_6(\mu_3\text{-}OH)(H_2O)_3](ClO_4)_2$, abbreviated as *tris*-$LnL_2$,[44] and the tetranuclear architecture, *tetra*-Ln_4L_9.

Experimental Section

Materials and Analytical Methods. Water sensitive reactions were carried out under an inert atmosphere (Ar) in oven-dried glassware. Unless otherwise stated, commercial grade solvents previously dried and deoxygenated by a solvent purification system based on alumina columns (Innov-Tech) were employed in the syntheses of the ligands and of the complexes. The starting chemical

(9) Gunnlaugsson, T.; Stomeo, F. *Org. Biomol. Chem.* **2007**, *5*, 1999.
(10) Piguet, C.; Bünzli, J.-C. G. *Chem. Rev.* **2002**, *102*, 2389.
(11) Tsukube, S.; Shinoda, M. *Chem. Rev.* **2002**, *102*, 1977.
(12) Mamula, O.; von Zelewsky, A. *Coord. Chem. Rev.* **2003**, *242*, 87.
(13) von Zelewsky, A.; Mamula, O. *J. Chem. Soc., Dalton Trans.* **2000**, 219.
(14) Mamula, O.; Lama, M.; Telfer, S.; Nakamura, A.; Kuroda, R.; Stoeckli-Evans, H.; Scopelitti, R. *Angew. Chem., Int. Ed.* **2005**, *44*, 2527.
(15) Mamula, O.; Lama, M.; Stoeckli-Evans, H.; Shova, S. *Angew. Chem., Int. Ed.* **2006**, *45*, 4940.
(16) Lama, M.; Mamula, O.; Kottas, G. S.; Rizzo, F.; De Cola, L.; Nakamura, A.; Kuroda, R.; Stoeckli-Evans, H. *Chem.—Eur. J.* **2007**, *13*, 7358.
(17) Jeong, K. S.; Kim, Y. S.; Kim, Y. J.; Lee, E.; Yoon, J. H.; Park, W. H.; Park, Y. W.; Jeon, S.-J.; Kim, Z. H.; Kim, J.; Jeong, N. *Angew. Chem., Int. Ed.* **2006**, *45*, 8134.
(18) Lehn, J.-M. *Chem.—Eur. J.* **1999**, *5*, 2455.
(19) Corbett, P. T.; Leclaire, J.; Vial, K.; Wietor, J.-L.; Sanders, J. K. M.; Otto, S. *Chem. Rev.* **2006**, *106*, 3652.
(20) Lehn, J.-M. *Proc. Natl. Acad. Sci. U.S.A.* **2002**, *99*, 4763.
(21) Senegas, J.-M.; Koeller, S.; Bernardinelli, G.; Piguet, C. *Chem. Commun.* **2005**, 2235.
(22) Yamamoto, T.; Arif, A. M.; Stang, P. J. *J. Am. Chem. Soc.* **2003**, *125*, 12309.
(23) Provent, C.; Rivara-Minten, E.; Hewage, S.; Brunner, G.; Williams, A. F. *Chem.—Eur. J.* **1999**, *5*, 3487.
(24) Mamula, O.; Monlien, F.; Porquet, A.; Hopfgartner, G.; Merbach, A. E.; von Zelewsky, A. *Chem.—Eur. J.* **2001**, *7*, 533.
(25) Kraus, T.; Budseinsky, M.; Cvacka, J.; Sauvage, J.-P. *Angew. Chem., Int. Ed.* **2006**, *118*, 264.
(26) Campos-Fernandez, C. S.; Schottel, B. L.; Chifotides, H. T.; Bera, J. K.; Bacsa, J.; Koomen, J. M.; Russell, D. H.; Dunbar, K. R. *J. Am. Chem. Soc.* **2005**, *127*, 12909.
(27) Albrecht, M.; Janser, J.; Runsink, J.; Raabe, G.; Weis, P.; Fröhlich, R. *Angew. Chem., Int. Ed.* **2004**, *43*, 6662.
(28) Scherer, M.; Caulder, D. L.; Johnson, D. W.; Raymond, K. N. *Angew. Chem., Int. Ed.* **1999**, *38*, 1588.
(29) Hasenknopf, B.; Lehn, J.-M.; Boumediene, N.; Van Dorsselaer, L. A.; Kneisel, D.; Fenske, D. *J. Am. Chem. Soc.* **1997**, *1198*, 10956.
(30) Schweiger, M.; Seidel, S. R.; Arif, A. M.; Stang, P. J. *Inorg. Chem.* **2002**, *41*, 2556.
(31) Lam, R. T. S.; Belenguer, A.; Roberts, S. L.; Naumann, C.; Jarrosson, T.; Otto, S.; Sanders, J. K. M. *Science* **2005**, *308*, 667.
(32) Hiraoka, S.; Fujita, M. *J. Am. Chem. Soc.* **1999**, *121*, 10239.
(33) Yamanoi, Y.; Sakamoto, Y.; Kusukawa, T.; Fujita, M.; Sakamoto, S.; Yamaguchi, K. *J. Am. Chem. Soc.* **2001**, *123*, 980.
(34) Ramirez, J.; Stadler, A.-M.; Kyritsakas, N.; Lehn, J.-M. *Chem. Commun.* **2007**, 237.
(35) Suzuki, K.; Kawano, M.; Fujita, M. *Angew. Chem., Int. Ed.* **2007**, *46*, 2819.
(36) Schalley, C. A.; Müller, T.; Linnartz, P.; Witt, M.; Schäfer, M.; Lützen, A. *Chem.—Eur. J.* **2002**, *8*, 3538.
(37) Fujita, M.; Ibukuro, F.; Hagihara, H.; Ogura, K. *Nature* **1994**, *367*, 720.
(38) Baxter, P. N. W.; Khoury, R. G.; Lehn, J.-M.; Baum, G.; Fenske, D. *Chem.—Eur. J.* **2000**, *6*, 4140.
(39) Park, S. J.; Shin, D. M.; Sakamoto, S.; Yamaguchi, K.; Chung, Y. K.; Lah, M. S.; Hong, J.-I. *Chem.—Eur. J.* **2005**, *11*, 235.
(40) Rodriguez, M.; Llobet, A.; Corbella, M.; Müller, P.; Usón, M. A.; Martell, A. E.; Reibenspeis, J. *J. Chem. Soc., Dalton Trans.* **2002**, 2900.
(41) Schuetz, S. A.; Day, V. W.; Rheingold, A. L.; Belot, J. A. *J. Chem. Soc., Dalton Trans.* **2003**, 4303.
(42) Pirondini, L.; Stendardo, A. G.; Geremia, S.; Campagnolo, M.; Samori, P.; Rabe, J. P.; Fokkens, R.; Dalacanale, E. *Angew. Chem., Int. Ed.* **2003**, *42*, 1384.
(43) Baum, G.; Constable, E. C.; Fenske, D.; Housecroft, C. E.; Kulke, T. *Chem. Commun.* **1998**, 2659.

(44) The name *tris*-LnL_2 is justified by the fact that the trinuclear structure is made up from three identical LnL_2 units.

Table 1. Selected Distances (in Å) within the 1st Coordination Sphere of Ln(III) Ions in *tetra*-Ln_4L_9 Complexes and Related *tris*-LnL_2 Structures

complex		COO set **S″**			bipyridine set **S″**		COO set **S‴**		COO set **S^{IV}**		bipyridine set **S^{IV}**		Ln−Ln	OH−Ln
Ln:	O21	O21	O22	N1	N2	O44	O43	O154	O155	N17	N18	O_{OH}	distances	trigonal plane
							tetra-$Pr_4[(+)\text{-}L]_9$							
Pr1	2.386(4)	2.536(4)	2.811(4)	2.664(6)	2.876(6)	2.461(5)	2.495(4)	2.458(5)				2.522(4)	4.0447(6)[a]	
Pr2	2.375(4)	2.525(4)	2.790(5)	2.644(6)	2.911(6)	2.436(4)	2.455(5)	2.436(4)				2.528(4)	4.0703(6)[b]	0.96(4)
Pr3	2.394(4)	2.502(4)	2.721(5)	2.654(6)	2.902(6)	2.435(5)	2.495(5)	2.445(4)				2.552(4)	4.0757(6)[c]	
Pr4									2.344(4)	2.652(6)	2.829(6)		6.0368(7)[d]	
									2.357(5)	2.674(6)	2.800(6)	4.605(4)	6.0597(8)[d]	
									2.363(5)	2.641(6)	829(6)		6.0158(7)[f]	
							tetra-$Nd_4[(-)\text{-}L]_9$							
Nd1	2.374(4)	2.519(4)	2.774(4)	2.643(4)	2.854(4)	2.435(4)	2.490(4)	2.440(4)				2.509(4)	4.019(2)[a]	
Nd2	2.362(4)	2.505(3)	2.760(4)	2.630(4)	2.895(5)	2.417(4)	2.448(4)	2.424(4)				2.514(4)	4.0457(6)[b]	0.96(4)
Nd3	2.373(3)	2.488(4)	2.706(7)	2.637(4)	2.879(4)	2.415(4)	2.480(4)	2.425(4)				2.537(4)	4.048(1)[c]	
Nd4									2.336(4)	2.642(4)	2.642(4)		6.019(2)[d]	
									2.326(4)	2.654(5)	2.776(4)	4.599(4)	6.046(2)[e]	
									2.346(4)	2.625(4)	2.802(4)		6.010(2)[f]	
							tetra-$Pr_4[(\pm)\text{-}L]_9$							
Pr1	2.376(7)	2.508(7)	2.721 (8)	2.629(9)	2.890(7)	2.421(7)	2.501(7)	2.467 (7)				2.513(6)	4.0741(8)[a]	
Pr2	2.392(5)	2.511(6)	2.724(9)	2.637(8)	2.90(1)	2.431(7)	2.498(6)	2.427(6)				2.541 (7)	4.0415(7)[b]	0.95(7)
Pr3	2.393(6)	2.527(6)	2.704(6)	2.645(7)	2.929(9)	2.429(5)	2.431(7)	2.449(6)				2.530(6)	4.0560(7)[c]	
Pr4									2.324(6)	2.633(6)	2.797(8)		5.9261(8)[d]	
									2.346(8)	2.66(1)	2.798(7)	4.569(7)	6.0154(9)[e]	
									2.349(6)	2.66(1)	2.814(9)		6.0433(9)[f]	
							tris-LnL_2							
Pr	2.356(6)	2.516(5)	2.701(6)	2.620(7)	2.827(7)	2.421(4)	2.395(5)					2.515(3)	4.0396(6)	0.943(8)
Nd	2.357(3)	2.516(4)	2.673(4)	2.612(4)	2.831(6)	2.394(4)	2.412(4)					2.510(2)	4.0337(4)	0.936(5)

[a] : Ln1-Ln2; [b] : Ln2-Ln3; [c] :Ln3-Ln1; [d] : Ln4-Ln1; [e] : Ln4-Ln2; [f] : Ln4-Ln3 distances.

Scheme 1. Divergent Self Assembly Leading to the Synthesis of Interconverting Trinuclear $[Ln_3\{(+)\text{-}L\}_6(\mu_3\text{-}OH)]^{2+}$ and Tetranuclear $[Ln_4\{(+)\text{-}L\}_9(\mu_3\text{-}OH)]^{2+}$ Complexes[a]

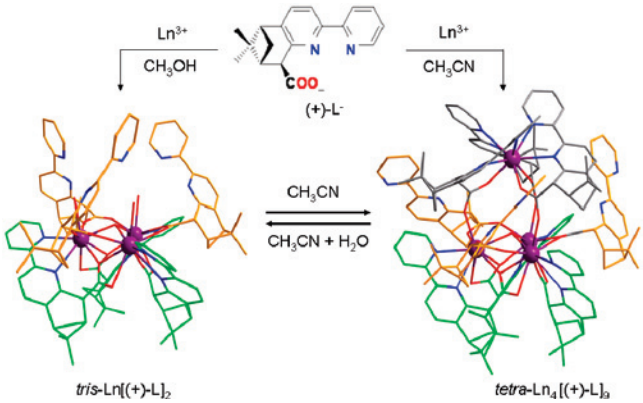

[a] The X-ray structures of Pr^{III} complexes are given as examples (views perpendicular to the C_3 axis).

compounds were purchased from Fluka (2-acetyl pyridine, >98%) and Aldrich (α-pinene, 99%, 97% *e.e.*). The Ln(III) perchlorate salts were prepared from the corresponding oxides according to literature procedure[45] (**Caution***! Perchlorate salts are potentially explosive*).[46,47] The concentrations of the stock solutions of $Ln(ClO_4)_3 \cdot xH_2O$ in MeOH were determined by complexometric titrations with $Na_2(H_2EDTA)$ and xylene orange as indicator.

The X-ray diffraction data were collected on an Oxford Diffraction CrysAlis CCD at 140(2) K and on a Stoe Mark II-IPDS at 173(2) K. The structures were solved by direct methods using SHEXLS-97,[48] and refined by the full-matrix least-squares on F^2 using SHELXL-97.[49] Hydrogen atoms were included in calculated positions and treated as riding atoms. Multiscan absorption corrections were applied for the complexes. Crystallographic data for the structure reported in this paper (cif file) is given in the Supporting Information.

Infrared spectra were collected in the range 4000−550 cm^{-1} with a Perkin-Elmer FT-IR Spectrum One provided with an ATR sampling accessory. ES-MS spectra were obtained with an instrument LCT from Waters-Micromass, combining an electrospray source and a TOF analyzer. Solutions of the metal complexes were diluted to 10^{-4} M, 10^{-5} M, and 10^{-6} M and injected by infusion at a flow rate of 5 μL/min. The ion spray voltage was set at 2600 V and 12V for the sample cone; source temperature = 120 °C. Spectra are the averaged result of one minute scan from m/z = 200 to 2500 at a rate of 1 scan/s. Deconvolutions have been performed using the Masslynx 3.4 software. The theoretical isotopic distribution was calculated by using the software ChemCalc.[50] ^{1}H- and ^{13}C-NMR spectra were registered on Bruker Avance 400 (400 MHz) and Bruker Avance 600 (600 MHz) spectrometers. The chemical shift values are referenced to TMS standard (0 ppm) while the residual proton impurities of the deuterated CD_3CN were used as internal reference.

Spectrophotometric Measurements. Suprasil quartz cells were used for all measurements. Spectrophotometric grade CH_2Cl_2 and CH_3CN were dried over CaH_2 and P_2O_5, respectively, and distilled under nitrogen prior to use. The solvents were transferred to dry, nitrogen-purged Schlenk flasks, and all subsequent transfers were performed under an atmosphere of nitrogen into dry, nitrogen-purged glassware.

The measurements at low temperature (77 K) were performed in quartz tubes inserted in a liquid-nitrogen filled quartz Dewar. UV−vis spectra were recorded on a Perkin-Elmer Lambda900 or

(45) Desreux, J. F. In *Lanthanide Probes in Life, Chemical and Earth Sciences. Theory and Practice.*; Bünzli, J-C. G. , Choppin, G. R. Eds.; Elsevier Science: Amsterdam, 1989.
(46) Raymond, K. N. *Chem. Eng. News* **1983**, *50*, 2.
(47) Wosley, W. C. *J. Chem. Educ.* **1973**, *50*, A335.
(48) Sheldrick, G. M. *Acta Crystallogr.* **1990**, *A46*, 467.
(49) Sheldrick, G. M. *SHEXLS-97, SHELXL-97, Programs for the Determination and Refinement of Crystal Structures*; University of Göttingen: Göttingen, Germany, 1997.
(50) Krompiec, M.; Patiny, L. *ChemCalc*; 2001; http://www.chemcalc.org/.

a Varian Cary 5000 double-beam UV−vis-NIR spectrometer and baseline corrected. Steady-state luminescence emission spectra were recorded on a HORIBA Jobin-Yvon IBH FL-322 Fluorolog 3 spectrometer equipped with a 450 W xenon arc lamp. Steady-state NIR measurements were performed using the Fluorolog 3 equipped with a peltier-cooled Hamamatsu H9170−75 (InP/InGaAs) PMT in the spectral range 930−1700 nm. Emission and excitation spectra were in all the cases corrected for source intensity (lamp and grating) and emission spectral response (detector and grating) by standard correction curves. Lifetimes for the europium and terbium complexes were recorded on the Fluorolog 3 using the FL-1040 phosphorescence module with a 70 W xenon flash tube (fwhm = 3 μs) with a variable flash rate (0.05−25 Hz). The signals were recorded on the TBX-4-X single-photon-counting detector and collected using a multichannel scaling (MCS) card in the IBH DataStation Hub photon counting module, and data analysis was performed using the commercially available DAS6 software (HORIBA Jobin Yvon IBH). The goodness of fit was assessed by minimizing the reduced chi squared function (χ^2) and visual inspection of the weighted residuals. Time-resolved NIR measurements were measured on an FL900CDT Time-Resolved T-Geometry Fluorometer equipped with a LTB MSG 400 nitrogen laser (337 nm; 20 μJ pulse energy, 10 Hz repetition rate) and a North Coast EO 817P liquid-nitrogen-cooled germanium detector with a time resolution of 0.3 μs. The signals were averaged using a digitized Tektronix oscilloscope and then analyzed using standard fitting software. Luminescence quantum yields (Φ_{em}) were measured on optically dilute solutions (absorbance value lower than 0.1 at excitation wavelength). Quantum yields for Eu(III) and Tb(III) complexes were determined relative to those of [Ru(2,2′-bipyridine)$_3$]Cl$_2$ (Φ_{em} = 1.6% in CH_3CN)[51] and to quininie bisulfate (Φ_{em} = 54.6% in 1N H_2SO_4),[52] respectively. Quantum yields for the Nd(III) complex were determined with respect to [Yb(TTA)$_3$·(H$_2$O)$_2$] as a standard (Φ_{em} = 0.35% in toluene).[53] The estimated errors are ±20% for the quantum yields and ±5% for the lifetime determinations.

Circular dichroism (CD) spectra were recorded with a Jasco J-810 spectrometer. The solutions (CH_3CN, CH_2Cl_2, c = 1 × 10^{-4} M) were thermostatted at 20.0 °C using a Jasco PFD-425S system.

Synthesis of [Ln$_4$L$_9$(OH)](ClO$_4$)$_2$. General Procedure. The syntheses were performed under inert atmosphere (Ar flux). Triethylamine (98 μL, 0.67 mmol, 2.3 equiv) was added to a solution of HL·HCl (100 mg, 29.5 mmol, 1 equiv) in CH_3CN (3 mL). A solution of Ln(ClO$_4$)$_3$·xH$_2$O (x = 2−4, [Ln] = 5 M, 0.44 equiv) in CH_3CN was then dropped onto the mixture. The reaction was stirred for 4−5 h before evaporating the solvent under reduced pressure. The recovered raw solid containing also the triethylammonium salts resulting from the reaction (vide infra) was dried in high vacuum (∼10^{-5} mbar). In the case of complexes with Pr(III), Nd(III), Sm(III), and Eu(III) the salts have been eliminated by washing the raw solid with cold MeOH under an inert atmosphere (N_2). During this step a part of the complex dissolved as well, leading to an important decrease of the virtually quantitative yield. In particular, it was impossible to isolate the pure complex with La(III), Gd(III), and Tb(IIII) compounds because of their high solubility in MeOH. Therefore, in these three cases the analyses were performed on the raw solids. Suitable crystals for X-ray analysis were grown in the case of Pr(III) and Nd(III) complexes after slow evaporation of dry CD_3CN solutions kept in desiccator.

[La$_4${(+)-L}$_9$(OH)](ClO$_4$)$_2$. ES-MS (10^{-4} M in CH_3CN): 1606.25 (100) [La$_4$(L)$_9$(OH)]$^{2+}$. ^{1}H NMR (400 MHz, CD_3CN, 20 °C): δ = 8.84 (d, $J_{1''',2'''}$ = 4.0 Hz, 1H, H(1′′′)), 8.56 (m, 2H, H(1^{IV}), H(4^{IV})), 8.43 (d, $J_{1'',2''}$ = 1.0 Hz, 1H, H(1′′)), 8.32 (d, $J_{4''',3'''}$ = 1.0 Hz, 1H, H(4′′′)), 8.29 (dd, $J_{2^{IV},3^{IV}}$ = 6.9 Hz, $J_{2^{IV},1^{IV}}$ = 5.0, 1H, H(2^{IV})), 8.20 (m, 2H, H(7′′′), H(4′′)), 8.17 (d, $J_{7^{IV},8^{IV}}$ = 7.5 Hz, 1H, H(7^{IV})), 8.11 (d, $J_{7'',8''}$ = 7.5 Hz, 1H, H(7′′)), 7.80 (dd, $J_{3'',2''}$ = 7.0 Hz, $J_{3'',4''}$ = 7.0 Hz, 1H, H(3′′)), 7.65 (d, $J_{8'',7''}$ = 7.5 Hz, 1H, H(8′′)), 7.47 (dd, $J_{2''',3'''}$ = 7.0 Hz, $J_{2''',1'''}$ = 5.0, 1H, H(2′′′)), 7.36 (dd, $J_{3''',2'''}$ = 6.5 Hz, $J_{3''',4'''}$ = 6.5 Hz, 1H, H(3′′′)), 7.30 (dd, $J_{3^{IV},2^{IV}}$ = 7.0 Hz, $J_{3^{IV},4^{IV}}$ = 7.0 Hz, 1H, H(3^{IV})), 7.22 (d, $J_{8^{IV},7^{IV}}$ = 7.5 Hz, 1H, H(8^{IV})), 7.20 (d, $J_{8''',7'''}$ = 7.5 Hz, 1H, H(8′′′)), 6.15 (d, $J_{2'',3''}$ = 7.0 Hz, 1H, H(2′′)), 3.93 (d, $J_{13'',12''}$ = 2.0 Hz, 1H, H(13′′)), 2.87 (m, 2H, H(13′′′), H(10′′)), 2.74 (d, 1H, $J_{13^{IV},12^{IV}}$ = 2.5 Hz, 1H, H(13^{IV})), 2.47 (bs, 1H, H(15b′′)), 2.42 (d, $J_{10''',15a'''}$ = 5.5 Hz, $J_{10''',15b'''}$ = 5.5, 1H, H(10′′′)), 2.36 (d, $J_{10^{IV},15a^{IV}}$ = 5.5 Hz, $J_{10^{IV},15b^{IV}}$ = 5.5 Hz, 1H, H(10^{IV})), 2.31 (under water peak, 1H, H(12′′)), 2.11 (d, $J_{15a^{IV},15b^{IV}}$ = 10.5 Hz, 1H, H(15a^{IV})), 1.46 (ddd, $J_{12,15b}$ = 6.0 Hz, $J_{12,10}$ = 6.0 Hz, $J_{12,13}$ = 2.5 Hz, 1H, H(12′′′)), 1.43 (ddd, $J_{12^{IV},15b^{IV}}$ = 6.0 Hz, $J_{12^{IV},10^{IV}}$ = 6.0 Hz, $J_{12^{IV},15b^{IV}}$ = 3.0 Hz, 1H, H(12^{IV})), 1.29 (s, 3H, Me 17′′), 1.17 (d, $J_{15a'',15b''}$ = 10.5 Hz, 1H, H(15a′′)), 1.12 (bs, 1H, H(15b′′′)), 1.09 (s, 3H, Me 17′′′), 0.80 (s, 3H, Me 17^{IV}), 0.67 (m, 2H, H(15b^{IV}), H(15a′′′)), 0.51 (s, 3H, Me 16′′), 0.31 (s, 3H, Me 16′′′), 0.09 ppm (s, 3H, Me 16^{IV}). ^{13}C NMR (CD_3CN, 100 MHz):δ = 179.3, 177.9, 177.3, 157.6, 157.4, 156.5, 156.3, 155.7, 154.7, 152.8, 152.4, 151.4, 150.5, 150.0, 148.5, 148.1, 145.8, 145.6, 141.3, 140.2, 137.9, 136.7, 136.6, 133.7, 125.8, 124.2, 124.0, 123.8, 123.3, 122.0, 121.8, 121.5, 120.2, 52.5, 51.3, 51.2, 46.4, 46.3, 46.1, 45.8, 43.2, 42.6, 42.1, 40.3 (2C), 30.5, 28.7, 28,4, 25.6, 25.0, 24.5, 21.5, 21.1, 20.9 ppm. UV−vis (λ_{max}, nm (ε, M^{-1}·cm^{-1})): 308 (108000), 271 (78000).

[Pr$_4${(+)-L}$_9$(OH)](ClO$_4$)$_2$. Yield after washing with MeOH: 45 mg (40%). Elemental analysis: Calcd (%) for $C_{108}H_{109}Pr_3N_{12}O_{24}Cl_2$·$H_2O$: C, 56.90; H, 4.54; N, 7.37. Found: C, 56.60; H, 4.55; N, 7.30. ES-MS (10^{-4} M in CH_3CN): 1609.42 (100) [Pr$_4$L$_9$(OH)]$^{2+}$. IR: 2931w (υ_{C-H} aliphatic), 1624s ($\upsilon_{as\ COO-}$), 1454w, 1427s and 1381s (υ_s COO^-), 1253w, 1232w, 1084s (υ Cl−O), 862w, 792m, 749m, 673m, 621m. ^{1}H NMR (400 MHz, CD_3CN, 20 °C): δ = 35.27 (bs, 1H, H(n.a.)), 31.70 (bs, 1H, H(15a′′′)), 19.90 (bs, 1H, H(na)), 14.67 (bs, 1H, H(12′′′)), 13.39 (d, $J_{8''',7'''}$ = 8 Hz, 1H, H(8′′′)), 13.05 (bs, 1H, H(15b′′′)), 12.90 (d, J = 7 Hz, 1H, H(1/4′′′)), 12.75 (d, $J_{7''',8'''}$ = 8 Hz, 1H, H(7′′′)), 10.15 (bs, 2H, H(10′′′) and H(15a′′)), 9.58 (d, J = 5 Hz, 1H, H(4/1′′′)), 9.05 (d, $J_{8^{IV},7^{IV}}$ = 7 Hz, 1H, H(8^{IV})), 8.74 (d, $J_{7^{IV},8^{IV}}$ = 7 Hz, 1H, H(7^{IV})), 8.09 (d, $J_{4^{IV},3^{IV}}$ = 8 Hz, 1H, H(4^{IV})), 7.40 (dd, $J_{3''',2'''}$ = 6 Hz, $J_{3''',4'''}$ = 5 Hz, 1H, H(2/3′′′)), 7.31 (bd, $J_{2'',3''}$ = 6 Hz, 1H, H(2′′)), 7.20 (dd, $J_{3^{IV},2^{IV}}$ = 7 Hz, $J_{3^{IV},4^{IV}}$ = 7 Hz, 1H, H(3^{IV})), 6.75 (bd, $J_{8'',7''}$ = 8 Hz, 2H, H(8′′) and (H3/2′′′)), 5.30 (s, 3H, Me 16′′′), 5.30 (d, $J_{2^{IV},3^{IV}}$ = 7 Hz, 1H, H(2^{IV})), 4.86 (dd, $J_{3'',2''}$ = 6 Hz, $J_{3'',4''}$ = 6 Hz, 1H, H(3′′)), 3.83 (s, 3H, Me 17′′′), 3.48 (bs, 2H, H(10′′) and H(15b′′)), 3.01 (bs, 1H, H(n.a.)), 2.58 (d, $J_{7'',8''}$ = 8 Hz, 1H, H(7′′)), 2.32 (bs, 1H, H(10^{IV})), 1.74 (d, $J_{4,3}$ = 8 Hz, 1H, H(4′′)), −0.11 (s, 3H, Me 17′′), −0.98 (s, 3H, Me 17^{IV}), −1.11 (bs, 1H, H(12′′)), −1.89 (bs, 1H, H(12^{IV})), −2.28 (s, 3H, Me 16^{IV}), −3.88 (s, 3H, Me 16′′), −4.40 (bs, 1H, H(n.a.)), −5.07 (bs, 1H, H(15a^{IV})), −6.20 (bs, 1H, H(15b^{IV})), −6.46 ppm (bs, 1H, H(n.a.)). Signals not assigned (n.a.) can be attributed to the following protons: H13′′, H13′′′, H13^{IV}, H1′′, and H1^{IV}. The attribution of H1′′′ and H4′′′ can be swapped, as well as H2′′′ and H3′′′. ^{13}C NMR (CD_3CN, 100 MHz): δ = 258, 180.6, 167.9, 167.0, 162.5, 162.2, 157.4, 154.3,

(51) Juris, A.; Balzani, V.; Barigelletti, F.; Campagna, S.; Belser, P.; von Zelewsky, A. *Coord. Chem. Rev.* **1988**, *84*, 85.
(52) Melhuish, W. H. *J. Phys. Chem.* **1961**, *65*, 229.
(53) Meshkova, S. B.; Topilova, Z. B.; Bolshoy, D. V.; Beltyukova, S. V.; Tsvirko, M. P.; Venchikov, Y. V.; Ya, V. *Acta Phys. Pol., A* **1999**, *95*, 983.

151.2, 150.3, 150.0, 148.7, 147.6, 145.9, 142.7, 142.6, 138.6, 136.2, 134.4, 132.5 (2 C), 130.5, 128.0, 125.8 (2 C), 125.3, 125.0, 124.5, 123.8, 123.5, 120.9, 120.1, 118.9, 76.4, 63.2, 60.0, 58.2, 54.7, 52.2, 47.7, 45.7, 44.3, 41.2, 38.5, 37.3, 36.3, 33.4, 29.4, 26.7, 23.7, 22.3, 22.1, 18.6, 18.0 ppm. UV−vis (λ_{max}, nm (ε, $M^{-1}\cdot cm^{-1}$)): 309(110000), 272(79000). CD (λ, nm ($\Delta\varepsilon$)): 327(287), 298(−35). $[\alpha]_D^{20} = 1250$ deg·dm²·mol⁻¹ (589 nm, $4.2\cdot10^{-3}$ M, CH_3CN). $[\alpha]_D^{20} = 1290$ deg·dm²·mol⁻¹ (589 nm, 4.1×10^{-3} M, CH_2Cl_2).

$[Pr_4\{(-)\text{-}L\}_9(OH)](ClO_4)_2$. Analyses identical as those reported for the enantiomer $[Pr_4\{(+)\text{-}L\}_9(OH)](ClO_4)_2$ (see above). CD (λ, nm ($\Delta\varepsilon$)): 327 (−285), 298 (37). $[\alpha]_D^{20} = -1297$ deg·dm²·mol⁻¹ (589 nm, 4.3×10^{-3} M, CH_2Cl_2).

$[Nd_4\{(-)\text{-}L\}_9(OH)(H_2O)_3](ClO_4)_2$. Yield after washing with MeOH: 43 mg (38%). Elemental analysis: Calcd(%) for $C_{162}H_{154}Nd_4N_{18}O_{27}Cl_2\cdot H_2O$: C, 56.35; H, 4.63; N, 7.22. Found: C, 56.38; H, 4.56; N, 7.31. ES-MS (10^{-4} M in CH_3CN): 1618.18 (100) $[Nd_4L_9(OH)]^{2+}$. IR: 2932w (υ_{C-H} aliphatic), 1626s ($\upsilon_{as\ COO^-}$), 1454w, 1428s (υ_s COO^-), 1380s, 1234w, 1085s (υ Cl−O), 862w, 791m, 752m, 678, 621m. ^{1}H NMR (400 MHz, CD_3CN, 20 °C): δ = 35.86 (bs, 1H, H(n.a)), 13.14 (bs, 1H, H(15a‴)), 11.24 (d, $J_{7''',8'''} = 8$ Hz, 1H, H(7‴)), 11.00 (d, $J = 7$ Hz, 1H, H(1/4‴)), 10.88 (bs, 1H, H(4″)), 10.50 (d, $J_{8''',7'''} = 8$ Hz, 1H, H(8‴)), 9.84 (d, $J = 5$ Hz, 1H, H(4/1‴)), 8.93 (d, $J = 5$ Hz, 1H, H(4^{IV})), 8.81 (bs, 1H, H(3″), 8.73 (d, $J_{7^{IV},8^{IV}} = 7$ Hz, 1H, H(7^{IV})), 7.88 (dd, $J_{3''',2'''} = 6$ Hz, $J_{3''',4'''} = 5$ Hz, 1H, H(2/3‴)), 7.77 (bs, 3H, H(8^{IV}) and H(2″) and H(12^{IV})), 7.51 (bs, 2H, H(3/2‴) and H(3^{IV})), 6.41 (d, $J_{8'',7''} =$ 8 Hz, 1H, H(8″)), 5.89 (bs, 2H, H(7″) and H(2^{IV})), 5.65 (bs, 1H, H(10‴)), 4.51 (bs, 1H, H(15b‴)), 4.16 (bs, 1H, H(12‴)), 3.73 (bs, 1H, H(15a″)), 2.82 (bs, 1H, H(n.a.)), 2.43 (bs, 2H, H(10^{IV}) and H($15a^{IV}$)), 2.33 (bs, 1H, H(10″)), 2.23 (s, 3H, Me 16‴), 2.10 (under solvent peak, 2H, H(15b″) and H(n.a.)), 1.87 (s, 3H, Me 17‴), 0.80 (s, 3H, Me 17^{IV}), −0.12 (s, 3H, Me 17″), −0.66 (bs, 2H, H($15b^{IV}$) and H(12″)), −1.06 (s, 3H, Me 16^{IV}), −2.13 (bs, 1H, H(n.a.)), −2.53 (bs, 1H, H(n.a.)), −2.82 ppm (s, 3H, Me 16″). Signals not assigned (n.a.) can be attributed to the following protons: H13″, H13‴, H13^{IV}, H1″, and H1^{IV}. The attribution of H1‴ and H4‴ can be swapped as well as H2‴ and H3‴. ^{13}C NMR (CD_3CN, 100 MHz): δ = 194.8, 181.7, 168.0, 160.7, 158.4, 153.2, 153.1, 151.9, 151.3, 150.5, 149.7 (2C), 147.5, 141.5, 138.9, 138.4, 137.7, 137.2, 136.3, 134.0, 133.8, 133.6, 131.5, 128.6, 128.4, 124.8, 124.6, 124.0, 122.6, 122.0, 108.7, 79.4, 70.8, 50.9, 48.9, 46.8, 46.5, 46.3, 45.8, 43.5, 40.6, 40.2, 39.9, 39.3, 38.1, 35.9, 30.3, 26.7, 26.2, 24.1, 23.6, 23.1, 20.0, 18.9 ppm. UV−vis (λ_{max}, nm (ε, $M^{-1}\ cm^{-1}$)): 309 (110 000), 270 (79 000). CD (λ, nm ($\Delta\varepsilon$)): 327 (−276), 298 (38). $[\alpha]_D^{20} = -1245$ deg·dm²·mol⁻¹ (589 nm, 3.7×10^{-3} M, CH_3CN); $[\alpha]_D^{20} = -1305$ deg·dm²·mol⁻¹ (589 nm, 4.0×10^{-3} M, CH_2Cl_2).

$[Sm_4\{(+)\text{-}L\}_9(OH)](ClO_4)_2$. Yield after washing with MeOH: 34 mg (30%). ES-MS (10^{-4} M in CH_3CN): 1630.03 (100) $[Sm_4L_9(OH)]^{2+}$. IR: 2934w (υ_{C-H} aliphatic), 1623m ($\upsilon_{as\ COO^-}$), 1454w, 1428m(υ_s COO^-), 1380m, 1234w, 1085s (υ Cl−O), 861w, 790m, 753m, 677, 622m. ^{1}H NMR (400 MHz, CD_3CN, 20 °C): δ = 13.52 (bs, 1H, H(1″)), 9.02 (d, $J_{1''',2'''} = 4$ Hz, 1H, H(1‴)), 8.72 (d, $J_{7''',8'''} = 8$ Hz, 1H, H(7‴)), 8.62 (d, $J_{4''',3'''} = 8$ Hz, 1H, H(4‴)), 8.25 (d, $J_{4^{IV},3^{IV}} = 8$ Hz, 1H, H(4^{IV})), 8.03 (dd, $J_{3^{IV},2^{IV}} = 8$ Hz, $J_{3^{IV},4^{IV}} = 8$ Hz, 1H, H(3^{IV})), 7.93 (m, 2H, H(3″) and H(7^{IV}), $J_{7^{IV},8^{IV}} = 8$ Hz), 7.85 (d, $J_{4'',3''} = 8$ Hz, 1H, H(4″)), 7.70 (m, 2H, H(1^{IV}) and H(8‴), $J_{8''',7'''} = 8$ Hz), 7.56 (d, $J_{7'',8''} = 8$ Hz, 1H, H(7″)), 7.53 (dd, $J_{2''',3'''} = 6$ Hz, $J_{2''',1'''} = 5$ Hz, 1H, H(2‴)), 7.37 (dd, $J_{3''',2'''} =$ 8 Hz, $J_{3''',4'''} = 8$ Hz, 1H, H(3‴)), 7.30 (d, $J_{8'',7''} = 8$ Hz, 1H, H(8″)), 7.11 (d, $J_{8^{IV},7^{IV}} = 8$ Hz, 1H, H(8^{IV})), 7.10 (1H, under H(8^{IV}) signal, H(2″)), 6.90 (dd, $J_{2^{IV},3^{IV}} = 7$ Hz, $J_{2^{IV},1^{IV}} = 5$, 1H, H(2^{IV})), 3.73 (bs, 1H, H(13″)), 3.65 (bs, 1H, H(13‴)), 2.87 (d, $J_{10''',15a'''} = 5$ Hz, $J_{10''',15b'''} = 5$, 1H, H(10‴)), 2.69 (d, $J_{10'',15a''} = 5$ Hz, $J_{10'',15b''} = 5$ Hz, 1H, H(10″)), 2.49 (d, $J_{15a''',15b'''} = 10$ Hz, 1H, H(15a‴)), 2.41(ddd, $J_{15b'',15a''} = 10$ Hz, $J_{15b'',10''} = 6$ Hz, $J_{15b'',12''} = 6$ Hz, 1H, H(15b″)), 2.27 (m, under water peak, 2H, H(13^{IV}) + H(10^{IV})), 2.11 (m, under water peak, 1H, H(12″)), 1.82 (bs, 1H, H(12‴)), 1.76 (bs, 1H, H(12^{IV})), 1.58 (d, $J_{15a'',15b''} = 10$ Hz, 1H, H(15a″)), 1.40 (bs, 1H, H(15b‴)), 1.16 (s, 3H, Me 17‴), 1.10 (s, 3H, Me 17″), 0.78 (s, 4H, H($15b^{IV}$) and Me 17^{IV})), 0.54 (s, 3H, Me 16‴), 0.05 (s, 3H, Me 16″), −0.25 (s, 3H, Me16^{IV}), −0.31 ppm (d, $J_{15a^{IV},15b^{IV}} = 7$ Hz, 1H, H($15a^{IV}$)). ^{13}C NMR (100 MHz, CD_3CN): δ = 184.8, 183.9, 171.5, 158.2, 157.8, 157.5, 156.8, 156.4, 153.9, 153.2, 152.0, 150.5, 150.3, 149.6, 144.9, 144.5, 143.3, 141.1, 140.3, 138.1, 136.3, 136.1, 134.5, 125.1, 124.2(2C), 123.3, 120.6, 120.3, 120.2, 118.4, 51.9, 49.8, 48.9, 47.4, 47.1, 46.9, 46.1, 45.8, 43.0, 42.5, 41.9, 40.2, 40.0, 30.3, 30.0, 27.8, 25.6, 24.8, 24.4, 21.4, 21.2, 20.8, 8.6 ppm. UV−vis (λ, nm (ε, $M^{-1}\ cm^{-1}$)): 308 (108000), 270 (80000). CD (λ, nm ($\Delta\varepsilon$)): 328 (283), 298 (−33). $[\alpha]_D^{20} = 1258$ deg·dm²·mol⁻¹ (589 nm, $3.6\cdot10^{-3}$ M, CH_3CN); $[\alpha]_D^{20} = 1302$ deg·dm²·mol⁻¹ (589 nm, 3.7×10^{-3} M, CH_2Cl_2).

$[Eu_4\{(+)\text{-}L\}_9(OH)](ClO_4)_2$. Yield after washing with MeOH: 47 mg (42%). Elemental analysis: Calcd (%) for $C_{162}H_{154}Eu_4N_{18}O_{27}Cl_2$: C, 56.17; H, 4.48; N, 7.28. Found: C, 56.20; H, 4.50; N, 7.18. ES-MS (10^{-4} M in CH_3CN): 1632.20 (100) $[Eu_4(L)_9(OH)]^{2+}$. IR: 2932w (υ_{C-H} aliphatic), 1630s ($\upsilon_{as\ COO^-}$), 1455w, 1428s (υ_s COO^-), 1384s, 1232w, 1084s (υ Cl−O), 864w, 792m, 749m, 673m, 622m. ^{1}H NMR (400 MHz, CD_3CN, 20 °C): δ = 10.81 (bs, 1H, H(n.a.), 10.67 (d, $J_{7'',8''} = 7$ Hz, 1H, H(7″)), 8.91 (bs, 1H, H(n.a.)), 8.74 (dd, $J_{3^{IV},2^{IV}} = 7$ Hz, $J_{3^{IV},4^{IV}} = 8$ Hz, 1H, H(3^{IV})), 8.60 (d, $J_{4,3} = 8$ Hz, 1H, H(4″)), 8.49 (d, $J_{8'',7''} = 7$ Hz, 1H, H(8″)), 8.28 (d, $J = 4$ Hz, 1H, H(1/4‴)), 7.93 (dd, $J_{2''',3'''} = 6$ Hz, $J_{2''',1'''} = 6$ Hz, 1H, H(2/3‴)), 7.83 (dd, $J_{3'',2''} = 7$ Hz, $J_{3'',4''} =$ 7 Hz, 1H, H(3″)), 7.58 (d, $J_{7^{IV},8^{IV}} = 8$ Hz, 1H, H(7^{IV})), 7.38 (dd, $J_{3''',2'''} = 5$ Hz, $J_{3''',4'''} = 7$ Hz, 1H, H(3/2‴)), 7.25 (d, $J_{4^{IV},3^{IV}} = 8$ Hz, 1H, H(4^{IV})), 6.95 (dd, $J = 8$ Hz, $J = 9$ Hz, 2H, H(2^{IV}) and H(4/1‴)), 6.30 (d, $J_{8^{IV},7^{IV}} = 8$ Hz, 1H, H(8^{IV})), 6.05 (d, $J_{7''',8'''} = 8$ Hz, 1H, H(7‴)), 5.73 (bs, 1H, H(12″)), 4.25 (d, $J_{8''',7'''} = 8$ Hz, 1H, H(8‴)), 3.00 (d, $J_{2'',3''} = 7$ Hz, 1H, H(2″)), 2.44 (s, 3H, Me16″), 2.34 (bs, 1H, H(10″)), 2.18 (bs, 1H, H($15a^{IV}$)), 1.72 (bs, 1H, H(15b″)), 1.68 (s, 3H, Me17″), 1.26 (s, 4H, Me16^{IV}), 1.13 (bs, 1H, H(10^{IV})), 0.63 (s, 3H, Me17^{IV}), 0.23 (bs, 1H, H($15b^{IV}$)), −0.01 (bs, 1H, H(12^{IV})), −0.26 (s, 3H, Me17‴), −1.05 (bs, 1H, H(10‴)), −1.24 (bs, 1H, H(n.a.)), −2.15 (s, 3H, Me16‴), −3.40 (d, $J_{15a'',15b''} =$ 10 Hz, 1H, H(15a″)), −3.74 (bs, 1H, H(15b‴)), −4.09 bs, 1H, H(n.a.)), −5.40 (bs, 1H, H(12‴)), −12.98(bs, 1H, H(n.a.)), −13.51 ppm (bs, 1H, H(15a‴)). Signals not assigned (n.a.) can be attributed to the following protons: H13″, H13‴, H13^{IV}, H1″ and H1^{IV}. The attribution of H1‴ and H4‴ can be swapped as well as H2‴ and H3‴. ^{13}C NMR (CD_3CN, 100 MHz): δ = 208.8, 171.3, 163.3, 161.1, 159.9, 156.4, 154.9, 152.7, 151.4, 151.2, 148.7, 147.6, 146.8, 143.8, 142.9, 142.0, 137.7, 134.0, 133.7, 133.4, 132.1, 129.6, 123.7, 118.5,114.1, 112.8, 112.2, 109.1, 108.3, 98.7, 97.9, 45.9, 47.5, 45.3, 44.4, 44.2, 43.5, 43.1, 41.6, 41.4, 41.0, 35.2, 28.4, 25.2, 24.8, 23.7, 23.2, 21.3, 20.4, 17.9, 11.4, −2.55 −11.0, −44.9 ppm. UV−vis (λ, nm (ε, $M^{-1}\cdot cm^{-1}$)): 309 (110 000), 272 (80 000). CD (λ, nm ($\Delta\varepsilon$)): 327 (278), 298 (−32). $[\alpha]_D^{20} = 1230$ deg·dm²·mol⁻¹ (589 nm, 3.6×10^{-3} M, CH_3CN). $[\alpha]_D^{20} = 1295$ deg·dm²·mol⁻¹ (589 nm, 3.8×10^{-3} M, CH_2Cl_2).

$[Gd_4\{(+)\text{-}L\}_9(OH)](ClO_4)_2$. ES-MS ($10^{-4}$ M in CH_3CN): 1642.50 (100) $[Gd_4(L)_9(OH)]^{2+}$. UV−vis (λ, nm (ε, $M^{-1}\cdot cm^{-1}$)): 308 (110 000), 272 (79 000).

$[Tb_4\{(+)\text{-}L\}_9(OH)](ClO_4)_2$. ES-MS ($10^{-4}$ M in CH_3CN): 1647.78 (100) $[Tb_4(L)_9(OH)]^{2+}$. UV−vis (λ, nm (ε, $M^{-1}\cdot cm^{-1}$)): 308 (110 000), 273 (78 000).

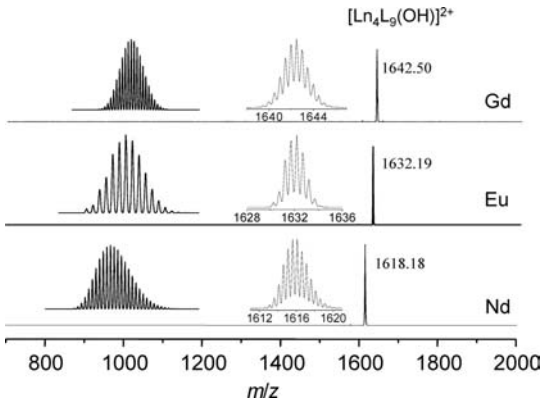

Figure 1. Selected ES-MS spectra of *tetra*-Ln_4L_9 (Ln = Nd, Eu, Gd, c ≈ 3×10^{-4} M, CH_3CN) and calculated patterns (on the left side).

Results and Discussion

Preparation and Solid State Characterization of *tetra*-Ln_4L_9. In-situ deprotonated ligand (+)- or (-)-L^- (2.25 equiv) was reacted successively with solutions of lanthanide perchlorate salts ($Ln(ClO_4)_3$, 1 equiv) in dry acetonitrile (see the Experimental Section).

The ES-MS analyses performed on the clear solutions obtained displayed, in the case of Ln(III) = La, Pr, Nd, Sm, Eu, Gd, and Tb, a single peak (Figure 1 and Supporting Information, Figure 1) with a *m/z* value and an isotopic distribution that can be undoubtedly assigned to a double-charged tetranuclear species with formula $[Ln_4L_9(OH)]^{2+}$. The general equation of the reactions can be written as follows:

$$9HL \cdot HCl + 4Ln(ClO_4)_3 \cdot xH_2O + 19Et_3N \rightarrow [Ln_4L_9(OH)](ClO_4)_2 + 9Et_3NHCl + 10Et_3NHClO_4 + (4x-1)H_2O$$

The ES-MS spectra of crude reaction mixtures with heavier Ln(III) ions (Dy, Ho, Er, Lu) show instead multiple signals but none corresponding to the above-mentioned tetranuclear formula. This second group was not further investigated, the attention being focused on those reactions leading to the tetranuclear species.

The triethyl ammonium salts resulting from the reactions were successively removed by washing the crude mixtures with cold methanol. The elemental analysis performed on the remaining precipitates confirmed their purity, in agreement with the general formula proposed after the ES-MS analysis. Thus, this procedure lead solely to the synthesis of the tetranuclear class of compounds $[Ln_4L_9(OH)](ClO_4)_2$ in their pure form, no traces of other compounds being found neither in solution nor in the solid state (vide infra). However, during this process a part of the tetranuclear species partially soluble in this solvent is also washed, lowering the virtually quantitative yield (40% for Ln = Pr, Nd, and Eu; 25% for Sm, see the Experimental Section). In the case of the tetranuclear complexes of La(III), Gd(III), and Tb(III), the rapid solubilization process prevented the isolation of salt-free samples.

Slow evaporation in an anhydrous environment of CD_3CN solutions of pure Pr(III) and Nd(III) complexes (with (+), (-)-L^-, respectively), afforded single crystals suitable for X-ray analysis. The cif file for the Nd(III) complex is given in the Supporting Information of this Article while the cif file for the Pr(III) was published as Supporting Information to the ref 15 (CCDC 607510). Two isostructural tetranuclear assemblies of general formula $[Ln_4L_9(\mu_3\text{-}OH)](ClO_4)_2 \cdot x CH_3CN$ (Pr(III): $x = 10$, (+)-L^-; Nd(III): $x = 4$, (-)-L^-) were revealed (Figures 2b, 2c, 3 and Scheme 1).

They display a tetranuclear core in which the four metal ions define the corners of a pseudotrigonal-pyramidal polyhedron (Figure 4). Three Ln(III) ions (Ln1, Ln2, and Ln3) constitute the pseudoequilateral triangle of the base (Ln−Ln distance ≈ 4 Å, see Table 1). A μ_3-hydroxide ion group lying on the pyramidal pseudo-C_3 axis (∼ 0.96 Å above the base) connects the three metals of the triangular base. The fourth Ln(III) (Ln 4) ion lies as well on the pseudo-C_3 axis, on the same side as the μ_3-OH group at about 5.55 Å above the metallic triangle. The pseudo-C_3 axis connects the nine ligands wrapping around the tetranuclear core in three distinct helical domains with predetermined configuration. The trinuclear base is held together by six bridging ligands that can be grouped into two sets: **S″** and **S‴** (Figures 2b and 2c and Figure 3). The coordination modes of these ligands are analogous to those observed in the related trinuclear complexes (Figures 2 and 4).

Three ligands forming the set **S″** (in green) bind two adjacent metal centers via the carboxylate group (in a μ^3-η^2:η^1 fashion) and via two bipyridine nitrogen atoms. The three ligands of the set **S‴** (in orange) are coordinating solely through the bridging carboxylate group in a symmetrical μ^2-η^1:η^1 fashion. As the bipyridine moieties of these latter ligands are not involved in coordination, they adopt the energetically more favorable *trans* conformation (Table 2). According to the chirality of the ligand, the helices individuated by the sets **S″** and **S‴** assume the same arrangements described in the case of *tris*-LnL_2 (Figure 2a). When a (+)-L^- is employed (as in the case of Pr(III) compound) the ligands of set **S″** and **S‴** adopt a *P* and *M* helical arrangement, respectively (Figure 3). The helicity is inverted by using the (-)-L^- enantiomer. The last three tridentate ligands (set $\mathbf{S^{IV}}$, gray) are coordinated to the top vertex of the trigonal pyramid through two nitrogen atoms from the bipyridine and one oxygen atom from the carboxylate group. Their helical arrangement around a single metal ion induces the configuration Λ at the stereogenic center when the (+)-L^- is used and the opposite Δ configuration when the (-)-L^- enantiomer is employed (Figure 3). This mononuclear subunit is connected to the trinuclear base via the oxygen atoms from the carboxylic groups belonging to the three ligands of the set $\mathbf{S^{IV}}$ (Figure 4).

The coordination number for each Ln(III) ion in the *tetra*-Ln_4L_9 structures is nine but the connectivity is different (Figure 4). The first coordination sphere of the three metal centers in the trigonal base presents two bipyridine nitrogens, six carboxylic oxygens, and one hydroxyl oxygen. The fourth center at the vertex of the pyramid is coordinated to six nitrogens (from the three bipyridines) and three carboxylic oxygens. Few slight differences in the distances Ln−X (X:

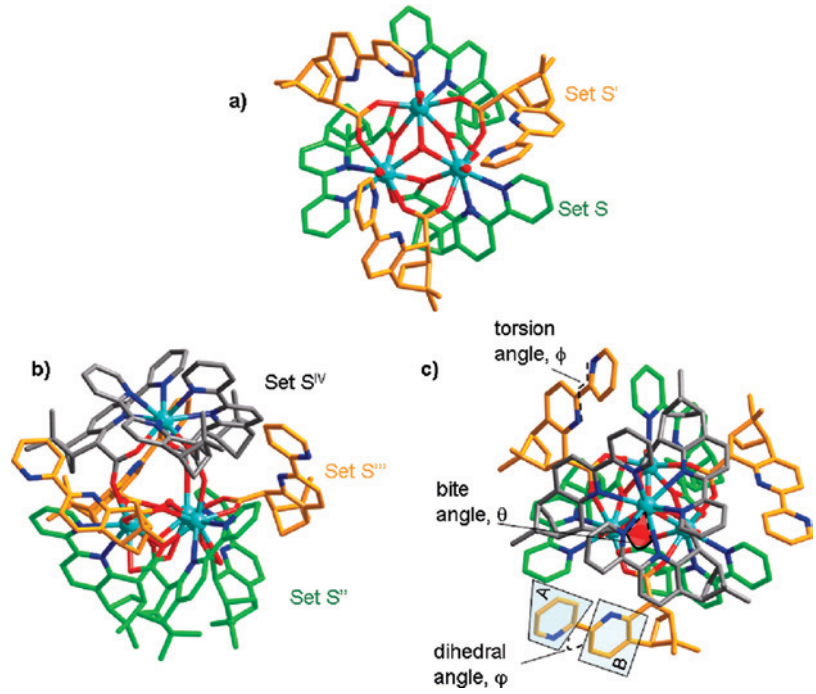

Figure 2. X-ray structures of (a) *tris*-Nd[(-)-L]$_2$, view parallel to the C_3 axis. Nd, turquoise; N, blue; O, red; ligands set **S**, light green; ligands set **S′**, orange. (b) *tetra*-Nd$_4$[(-)-L]$_9$, view perpendicular to the C_3 axis. Ligands set **S″**, light green; set **S‴**, orange; set **S^{IV}**, gray. (c) *tetra*-Nd$_4$[(-)-L]$_9$, view parallel to the C_3 axis. In evidence, the selected angles reported in Table 2.

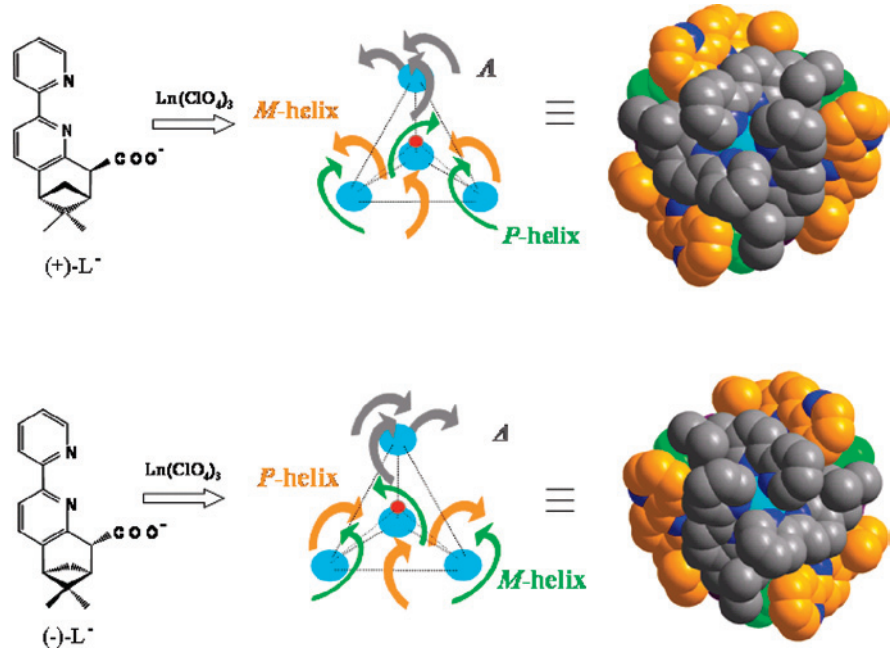

Figure 3. Helical arrangement of the three sets of ligands around the metal centers in *tetra*-Ln$_4$L$_9$ structures, using the (+) or the (−) enantiomer of the ligand. Green arrows, set **S″**; orange arrows, set **S‴**; gray arrows, set **S^{IV}**.

atom in the first coordination sphere) are pointed out comparing the values reported for the trinuclear subunit of the *tetra*-Pr$_4$[(+)-L]$_9$ complex with the distances in the corresponding discrete *tris*-PrL$_2$ structures (Table 1). Some of the bond lengths are indeed longer in the *tetra*-Ln$_4$L$_9$ structure. In particular, this concerns the distance Ln−O43 of the carboxylic oxygen in the ligands of set **S′** (Ln: Pr = 2.39 Å, Nd = 2.41 Å) increasing up to 2.49 Å in both *tetra*-Pr(III) and -Nd(III) complexes. The ligands of set **S′** coordinate only through their carboxylic moiety in a bridging fashion. The coordination of the sterically hindered mononuclear subunit in the *tetra*-Ln$_4$L$_9$ complexes provokes a flattening of these bidentate bridging ligands which results in the elongation of the coordinative bonds. The coordinative bonds of a carboxylic oxygen (O22) and a bipyridine nitrogen (N16) from ligands of set **S** are affected as well upon coordination of the mononuclear subunit. In the *tetra*-Ln$_4$L$_9$ structures the distances Ln−O22 and Ln−N16 are again longer (Ln = Pr, 2.81 and 2.91 Å; Nd, 2.77 and 2.89 Å, respectively) than the distances measured in the *tris*-LnL$_2$

Table 2. Selected Angles of the Bipyridine Moieties within the Three Ligands Sets of *tetra*-Ln_4L_9 Structures[a]

	set	bite angle (deg)	dihedral angle (deg)	torsion angle (deg)
tetra-Pr_4[(+)-L]$_9$	**S‴**	59.5(2) 59.6(2) 59.7(2)	11.9(2) 12.9(2) 12.1(2)	2.3(8) 3.3(9) 10(1)
	S‴		5.2(3) 2.4(4) 16.8(3)	177.4(6) 179.2(8) 167.1(7)
	S^{IV}	60.5(2) 61.5(3) 60.6(1)	13.1(3) 11.4(3) 9.2(4)	6(1) 7(1) 2(1)
tetra- Nd_4[(-)-L]$_9$	**S‴**	59.7(1) 60.2(1) 59.7(2)	12.2(2) 12.3(2) 12.8(2)	2.5(7) 3.1(7) 7.6(7)
	S‴		5.6(2) 2.1(2) 12.2(2)	175.2(5) 165.5(6) 179.3(7)
	S^{IV}	60.8(3) 61.6(2) 61.1(3)	9.5 (2) 13.9(2) 11.7(2)	6.5(7) 8.3(7) 1.1(7)
tetra-Pr_4[(±)-L]$_9$				
	S‴	59.5(2) 59.6(2) 59.7(2)	11.9(2) 12.9(2) 12.1(2)	2.3(8) 3.3(9) 10(1)
	S‴		5.2(3) 2.4(4) 16.8(3)	177.4(6) 179.2(8) 167.1(7)
	S^{IV}	60.5(2) 61.5(3) 60.6(1)	13.1(3) 11.4(3) 9.2(4)	6(1) 7(1) 2(1)

[a] See the Figure 2c for the definition of the angles.

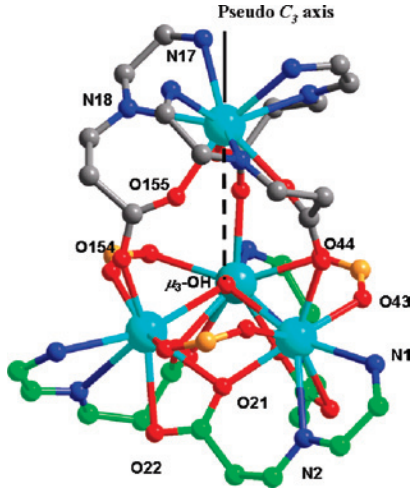

Figure 4. Pyramidal metallic framework of the *tetra*-Pr_4[(+)-L]$_9$ structure with the coordination sites of the ligands in the three sets. In evidence, the nine bridging carboxylic groups.

complexes (Ln = Pr, 2.70 and 2.83; Nd, 2.67 and 2.83 Å, respectively). As in the case of *tris*-LnL_2 structures, the geometry of the coordination polyhedra around the Ln(III) ions in the *tetra*-Ln_4L_9 structures is intermediate between the capped square antiprism and the tricapped trigonal prism. Only a computational shape analysis could eventually state which idealized geometry matches more closely the experimental results.[54]

IR spectra of *tetra*-Ln_4L_9 complexes measured on crystals and purified amorphous solids were found identical and represent another clear proof of isostructurality (Supporting Information, Figure 2). The spectra present a high frequency domain (3500−3000 cm^{-1}) void of the large band characteristic of the H−O−H stretching observed in *tris*-LnL_2 complexes. This is due to the loss of water molecules in the first coordination sphere in *tetra*-Ln_4L_9 complexes. Nevertheless, the band arising from ν(OH) around 3550 cm^{-1} is still present and is attributed to the group μ_3-OH. Another intense band at 1082 cm^{-1} corresponds to the stretching vibration of the ClO_4^- counterion, accounting for unbound perchlorate anions.[55] The symmetric and asymmetric stretching modes of the O−C−O bonds in the carboxylic function are revealed by the characteristic strong bands in the region 1630−1350 cm^{-1}. In particular, overlapping bands corresponding to $\nu(COO)_{as}$ are observed around 1625 cm^{-1}, while two distinct bands for $\nu(COO)_s$ are found around 1425 and 1380 cm^{-1}. This leads to differences $\Delta(\nu_{as} - \nu_s)$, respectively, of 200 and 245 cm^{-1} that can be related to a bidentate cyclic and to a bidentate-bridging coordination mode of the carboxylate groups.[56,57] The X-ray structure confirms these coordination modes as they are characteristic for ligands of set **S″** (bidentate cyclic) and sets **S‴** and **S^{IV}** (bidentate-bridging).

Solution Studies of *Tetra*-Ln_4L_9 Complexes. The analysis of ^{1}H NMR spectra was limited to the diamagnetic or low paramagnetic complexes formed with Ln(III) = La, Pr, Nd, Sm, and Eu. The ^{1}H NMR spectra measured in CD_3CN and CD_2Cl_2 display a total of 39 resonances each, accounting for an averaged C_3 symmetry on the NMR time scale. The signals can be grouped into three groups of equal intensity ascribed to the three sets of ligands observed in the solid state and displaying 13 signals each. The line assignment was achieved by two-dimensional ^{1}H−^{1}H analysis (COSY and ROESY) and is presented in Figure 5 (for Nd(III) complex) and resumed in the Supporting Information, Table 1. In particular, ROESY spectra provided decisive information to group the signals into the three sets. The *intra*-ligand cross peak H4/H7 is indicative for a *cis* conformation of the bipyridine rings. Considering the connectivity of the different ligands in *tetra*-Ln_4L_9 structures, this ROESY contact should be detected only in the case of set **S″** and set **S^{IV}**. The bipyridine moieties coordinate the metal centers through both the nitrogen atoms, adopting consequently the *cis* conformation. The absence of the H4/H7 cross peak in the case of set **S‴** indicates a *trans* conformation for these ligands which bind just through the carboxylic moiety.

The ROESY spectra afforded as well a series of *inter*-ligand cross peaks. The highest number of NOE contacts was detected in the better resolved spectra of the diamagnetic *tetra*-La_4[(+)-L]$_9$ complex (20) and of the weakly paramagnetic *tetra*-Sm_4[(+)-L]$_9$ complex (18). Up to nine common cross peaks are identified for all the complexes (Supporting Information, Table 2), providing an important proof of the isostructurality of all the *tetra*-Ln_4L_9 complexes in solution. Moreover, a further comparison of the interligand NOE contacts with the solid state H−H distances extracted from X-ray data, confirmed that the *tetra*-Ln_4L_9 structure observed in solid state is retained in solution (Supporting Information,

(54) Xu, J.; Radkov, E.; Ziegler, M.; Raymond, K. N. *Inorg. Chem.* **2000**, *39*, 4156.
(55) Bünzli, J.-C. G.; Yersin, J.-R.; Mabillard, C. *Inorg. Chem.* **1982**, *21*, 1471.
(56) Deacon, G. B.; Phillips, R. J. *Coord. Chem. Rev.* **1980**, *33*, 227.
(57) Nakamoto, K. *Infrared and Raman Spectra of Inorganic and Coordination Compounds*; Wiley-Interscience: New York, 1990.

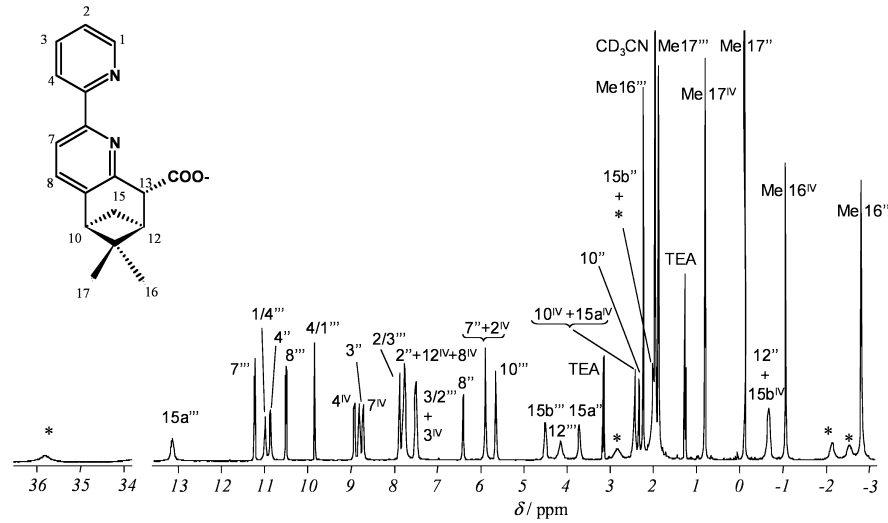

Figure 5. Attributed ^{1}H NMR spectrum of *tetra*-Nd_4[(-)-L_9] (CD_3CN, room temperature (rt), c = 8 × 10^{-3} M).

Figure 3). Because only *tetra*-Nd_4[(-)-L]$_9$ and -Pr_4[(+)-L]$_9$ X-ray data were available, these were used to compare ROESY data of all the complexes, assuming that only small differences existed in the distances among protons in the different solid state structures. In Nd(III), Pr(III), and Eu(III) complexes some signals have lost their couplings because of the fast relaxation induced on the corresponding nuclei by paramagnetic centers and could not be unequivocally assigned. It is the case of the protons lying in proximity of the coordinative sites of the ligands (labeled with ∗ in Figure 5) and in particular H1 in sets **S″** and **S^{IV}** and H13 in all the three sets.

^{13}C NMR spectra on the same samples confirm the data from ^{1}H NMR analysis. A total of 54 peaks are observed and correspond to three sets of signals, each one accounting for 18 resonances from one single set of equivalent ligands.

To simplify the ^{13}C NMR spectra, a ^{13}C-marked derivative of the ligand was synthesized. The ^{13}C was introduced at the level of the carboxylic moiety, thus marking one of the binding sites of the molecule by reacting using marked $^{13}CO_2$ in the last step of the ligand synthesis. The ^{13}C NMR spectrum of a *tetra*-Pr_4[(+)-L]$_9$ complex synthesized with this ^{13}C-marked ligand displayed only three signals at 258.2 167.5 and 167.0 ppm. (Supporting Information, Figure 4). Instead, in the case of related Pr(III) trinuclear complex, only two resonances corresponding to sets **S** and **S′**, respectively, were detected.[15]

Photophysical and Chiroptical Properties. All the *tetra*-Ln_4L_9 complexes show the same absorption profiles, featuring a major band located at 32 350 cm^{-1} (309 nm) that displays two additional shoulders around 33 000 and 31 000 cm^{-1}. These bands can be ascribed to the $\pi \rightarrow \pi^*$ transitions mainly located on the pyridine units and undergo a red-shift of 1800 cm^{-1} from the position in the spectrum of the anionic form of the free ligand, L^- (34 150 cm^{-1}, 293 nm). This accounts for the *trans*→*cis* isomerization of the bipyridine moiety upon complexation. Three additional bands are observed at higher energies, in the region 39 000−37 500 cm^{-1} (Supporting Information, Figure 4). The ε values are consistent along the series (Ln = La, Pr, Nd, Sm, Eu, and Tb) and confirm the presence of nine ligands per complex: the absorbance value ε_{309} = 109 000 M^{-1} cm^{-1} recorded in the case of tetranuclear complexes is approximately nine times higher than the value ε_{293}= 13 000 M^{-1} cm^{-1} recorded in the case of the free anionic ligand.

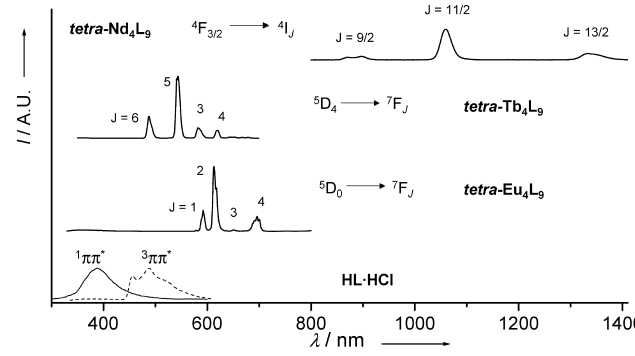

Figure 6. Emission spectra of ligand HL·HCl and the visible- and NIR-emitting *tetra*-Ln_4L_9 complexes in CH_2Cl_2 measured at rt (solid line, [L] = 5 × 10^{-5} M, [LnL] ≈ 1·10^{-6} M), and 77 K (dotted line, time delay = 0.05 ms).

The band corresponding to the singlet state ($^1\pi\pi^*$) emission of the ligand appears around 25 850 cm^{-1} (387 nm) upon excitation of a ligand solution in dichlorometane (λ_{ex} = 275 nm), as shown in Figure 6. The triplet state emission ($^3\pi\pi^*$) is revealed at 77 K at 20 500 cm^{-1} (488 nm) and appears as a band structured in a vibrational progression of 1500 ± 50 cm^{-1}, with the 0-phonon transition at 21 950 cm^{-1} (456 nm).

Upon excitation at 275 nm of dichloromethane solutions, both the *tetra*-Eu_4[(+)-L]$_9$ and *tetra*-Tb_4[(+)L]$_9$ complexes display bright and characteristic metal-centered luminescence (Figure 6). An extremely faint ligand-centered emission is still detected in these spectra, indicating that either energy transfer between the ligand and the metal center is nearly quantitative or that there is some degree of ligand dissociation at low concentration (10^{-5}−10^{-6} M). Quantum yields of 9% were measured for both the compounds.

The emission of the two complexes is characterized by a monoexponential decay with lifetimes of 1.7 and 0.67 ms for Eu(III) and Tb(III), respectively (Table 3). These values

Table 3. Ligand- and Metal-Centered Emission Properties of (+)-H_2L^+ and Its *tetra*-Ln_4L_9 Complexes (Ln = Eu, Tb, Nd) in CH_2Cl_2[a]

compounds	$E(^1\pi\pi^*)$/cm^{-1}	$E(^3\pi\pi^*)$/cm^{-1}	E (^5D_J) [h]/cm^{-1}	ΔE (0-phonon $^3\pi\pi^*$ - ^5D_J)/cm^{-1} [g]	τ/ms	Q_L^{Ln}/%
H_2L^+	19400−32500 *25850*	16350−22900 large *20500* **21950**				
tetra-Eu_4L_9	22200−30300 *27900*		17300 (579 nm)	4650	1.7 [b]	9 [d]
tetra-Tb_4L_9	23800−30600 *28250*		20500 (488 nm)	1450	0.67 [c]	9 [e]
tetra-Nd_4L_9					0.50 [f]	0.1 [g]

[a] Maxima indicated in italic, 0-phonon levels in bold. [b] Measured at rt, on the $^5D_0 \rightarrow {}^7F_2$ transition (615 nm). [c] Measured at rt, on the $^5D_4 \rightarrow {}^7F_5$ transition (540 nm). [d] Calculated with respect to $Ru(bpy)_3$ ($Q_r = 1.6\%$ in CH_3CN). [e] Calculated with respect to quininie bisulfate ($Q_r = 54.6\%$ in 1N H_2SO_4). [f] Measured at rt, on the $^4F_{3/2} \rightarrow {}^4I_{11/2}$ transition (1063 nm). [g] Calculated with respect to $[Yb(TTA)_3 \cdot (H_2O)_2]$ ($Q_r = 0.35\%$ in toluene). [h] $J = 0$ for *tetra*-Eu_4L_9 and 4 for *tetra*-Tb_4L_9.

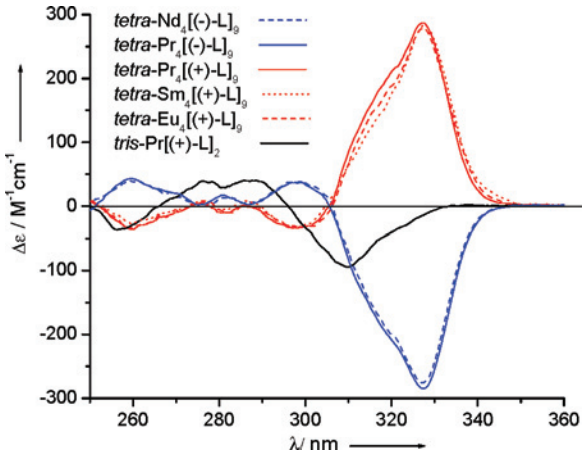

Figure 7. CD spectra of pure *tetra*-Ln_4L_9 complexes (CH_3CN, c = 1 × 10^{-4} M, rt). The CD spectrum of the trinuclear *tris*-Pr[(+)-L]$_2$ compounds is also reported for comparison.

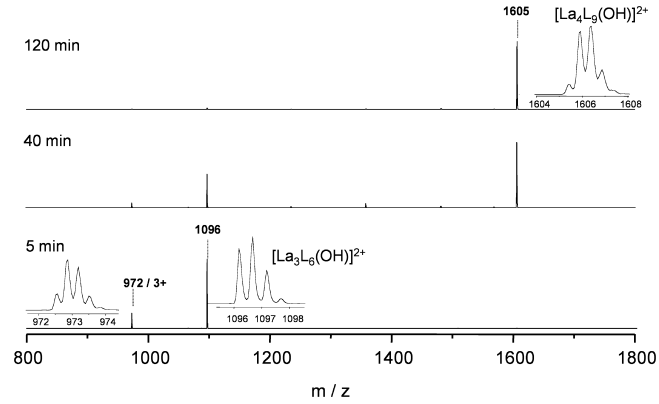

Figure 8. Evolution of the ES-MS spectra of *tris*-La[(+)-L]$_2$ in CH_3CN (c ≈ 3 × 10^{-4} M).

are relatively high and compatible with the absence of O−H oscillators in the first coordination sphere (excluding the μ_3-OH group).[58,59] Under the same conditions, *tetra*-Nd_4[(-)-L]$_9$ displayed a NIR luminescence in the region 840−1400 nm, with the main band ($^4F_{3/2} \rightarrow {}^4I_{11/2}$) centered at 1063 nm (Figure 6). To quantify the ability of the ligand to sensitize the NIR-emitting Nd(III), the quantum yield was determined ($\Phi_{Nd} = 0.10\%$). The luminescence decay is again monoexponential and the corresponding lifetime measured on the $^4F_{3/2} \rightarrow {}^4I_{11/2}$ transition is 0.50 μs (Table 3).

CD spectra recorded on *tetra*-Pr_4L_9 solutions in CH_3CN (c ≈ 10^{-4} M), with Ln(III) = Pr, Nd, Sm, and Eu are presented in Figure 7.

A strong activity is displayed in the region 300−340 nm, with maximum centered at 327 nm, in correspondence to the absorption maximum of the π-π transition of bipyridine. As representative of the CD profile of *tris*-LnL_2 compounds, the spectrum of *tris*-Pr[(+)-L]$_2$ is reported for comparison. Considering the absolute value of $\Delta\varepsilon$, *tetra*-Ln_4L_9 complexes display values about 1.7 times higher than *tris*-LnL_2. More important is, however, the change in sign of this band when going from a trinuclear to a tetranuclear structure with the same enantiomer of the ligand. Because the unit Ln_3L_6 is the same in the two complexes, the change in sign and intensity of the CD profile can be ascribed to the decisive contribution brought by the new LnL_3 subunit. The wrapping of these ligands around one metal center (set **S^{IV}**) describes an opposite helix than the ligands of set **S″** wrapping around the trimetallic core. Therefore the effect of the internuclear exciton coupling among the ligands **S″**[16] is outweighed by the opposite effect of the intranuclear exciton coupling of ligands of set **S^{IV}** within the mononuclear subunit. The contribution brought by the ligands of set **S‴** binding only through their carboxylic moieties can be neglected, as explained for the ligands **S′** of *tris*-LnL_2 complexes (see above). The interchromophore separation among the three ligands of set **S^{IV}** in the mononuclear subunit of *tetra*-Ln_4L_9 compounds (Ln = Pr: 5.80 Å; Nd: 5.72 Å) is smaller than among the ligands of set **S‴** in the trinuclear subunit (Ln = Pr, 9.66 Å; Nd, 9.61 Å). As a result, the amplitude of the Cotton effect arising from the coupling of two chromophores (which is inversely proportional to r^2)[60] is larger in the case of the LnL_3 subunit rather than for the trinuclear one. This leads to the inversion in sign of the main band in the spectrum of *tetra*-L_4nL_9 complexes with respect to *tris*-LnL_2. Otherwise, as expected, the complexes synthesized with opposite enantiomers of the ligand give rise to mirror image CD spectra. This is illustrated, for instance, in the case of *tetra*-Pr_4[(+)-L]$_9$ and *tetra*-Pr_4[(-)-L]$_9$ spectra.

Chiral Recognition. The self-assembly leading to *tris*-LnL_2 species displayed a high extent of chiral self-recognition.[15,16] To study the chiral recognition capabilities of the

(58) Quici, S.; Cavazzini, M.; Marzanni, G.; Accorsi, G.; Armaroli, N.; Ventura, B.; Barigelletti, F. *Inorg. Chem.* **2005**, *44*, 529.
(59) Kottas, G. S.; Mehlstäubl, M.; Fröhlich, R.; De Cola, L. *Eur. J. Inorg. Chem.* **2007**, 3465.
(60) Harada, N.; Chen, S.-M. L.; Nakanishi, K. *J. Am. Chem. Soc.* **1975**, *97*, 5345.

more complex tetranuclear system, we reacted an artificial racemic mixture of the ligand in acetonitrile under dry conditions, with $Pr(ClO_4)_3$ in proportions M/L 2:2.25, in the presence of base. The ^1H NMR spectrum obtained was very complicated (Supporting Information, Figure 5). Signals attributed to the *tetra*-Ln_4L_9 species are, however, present but in low amount. The other, major signals correspond to unassigned species and indicate that the tetranuclear assembly, which is obtained quantitatively when the enantiomerically pure (+)-L^- ligand is used, is in this case a minor part of a complicated mixture. In the case of the *tris*-LnL_2 system, the presence of the racemic ligand did not perturb the self-assembly, showing that the chiral recognition capabilities are effective for a given number of fundamental components (metal ions and ligands, nine in that case). When this number is higher (13, for the tetranuclear complexes), errors in the chiral recognition drastically affect the results of the self-assembly process.

Reversible Switching between Trinuclear and Tetranuclear Architectures in Solution. The trinuclear and the tetranuclear superstructures are the discrete products of two self-assembly processes from the same constituents (Ln(III) ions and ligand) taking place in two different solvent systems. If the reaction is performed in methanol, trinuclear structures $[Ln_3L_6(OH)(H_2O)_3](ClO_4)_2$ are obtained quantitatively. If the same components are self-assembling in acetonitrile, tetranuclear compounds $[Ln_4L_9(OH)](ClO_4)_2$ are exclusively obtained. The solvent is thus crucial in these chemical systems, and two further observations prompted us to study the "switchability" properties of these species in solution. First, it was observed by various techniques (vide infra) that the trinuclear arrays which are stable in weakly polar solvents (CH_2Cl_2) underwent an evolution in time in the more polar acetonitrile. Second, the tetranuclear architecture, which is stable both in CH_2Cl_2 and in *anhydrous* acetonitrile, can be modified in this latter solvent simply by adding small amounts of water. These initial observations were confirmed by different spectroscopic techniques (ES-MS, NMR and CD) along the Ln series.

The dissolution of pure trinuclear species in acetonitrile lead to mixtures in which the main product is the tetranuclear architecture. The general equation of the transformation can be written as follows:

$$a\left[Ln_3L_6(OH)(H_2O)_3\right](ClO_4)_2 \underset{CH_3CN + H_2O}{\overset{CH_3CN}{\rightleftharpoons}} b\left[Ln_4L_9(OH)\right](ClO_4)_2 + \left\{cLn^{3+} + dL^- + eOH^- + fClO_4^- + 3aH_2O\right\}$$

where $c = 3a - 4b$, $d = 6a - 9b$, $e = a - b$, and $f = 2a - 2b$. It was impossible to determine the exact formula of the species accompanying the tetranuclear compound (indicated generically as "minor species"). For this reason in the above equation the components making up the minor species are written in italics between the brackets.

Moreover, this conversion was found to be reversible in presence of water, pointing out the potentialities of a facile switch between these structures with variable nuclearity. Various factors (lanthanide ionic radius, concentration, enantiomeric purity) influencing the switching process have been studied in detail (vide infra).

The behavior of solutions of *tris*-LnL_2 (Ln = La, Pr, Nd, Eu, Gd, Tb, Dy, Er) in dry acetonitrile (10^{-4} M) was first monitored with a series of time dependent ES-MS experiments. In the spectra of equilibrated La(III) (Figure 8) and Pr(III) samples, the peak corresponding to the *tetra*-Ln_4L_9 species appears as the most intense, while the signal of the trinuclear species is at the limit of the detection.

In the spectra of Pr(III), Nd(III), Sm(III), Gd(III), and Tb(III) complexes an additional peak is detected respectively at m/z = 727, 731, 736, 744, and 745 corresponding to the fragment $[Ln_nL_{2n}]^{n+}$ (with n varying from 1 to 4) probably related to the minor species developing during the conversion (Supporting Information, Figure 6). For heavier lanthanides (Ln(III) = Eu, Gd, Tb, Dy) the main peak corresponds to the trinuclear species. Here the peak corresponding to the tetranuclear core is less intense pointing out a limited trinuclear to tetranuclear conversion. In the case of Er(III)—the last and the heaviest member of the trinuclear lanthanide class—this conversion is no longer observed. The spectrum does not present any change even a few days after dissolution and shows only the molecular cation peak corresponding to the *trinuclear* species.

The employment of *tris*-LnL_2 complexes synthesized with a ^{13}C-marked ligand allowed us to conveniently follow the

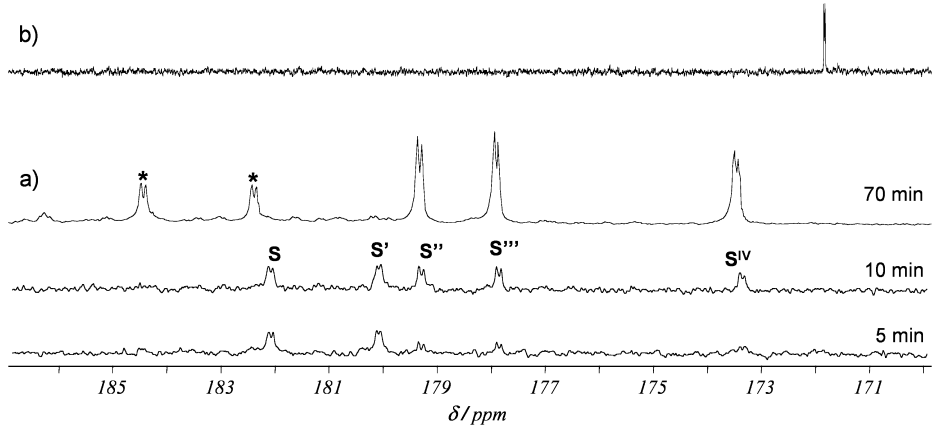

Figure 9. (a) Evolution of the ^{13}C NMR spectrum upon conversion of ^{13}C marked *tris*-La[(+)-$L]_2$ in CD_3CN (7.2×10^{-3} M, rt). The times reported are intended for after dissolution of the *tris*-LnL_2 complex. *: signals corresponding to minor unassigned species. (b) Spectrum of the ^{13}C-marked (+)-HL·HCl in CD_3CN.

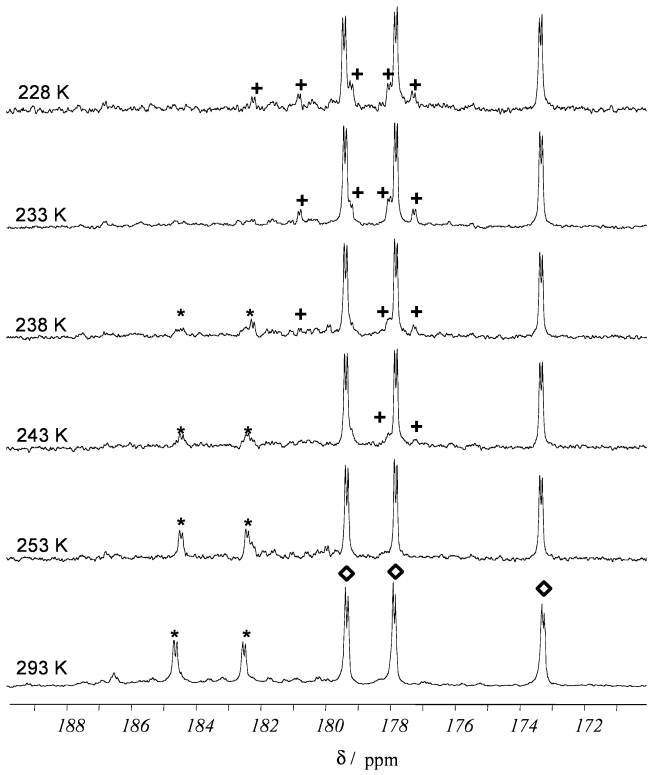

Figure 10. Temperature dependent ^{13}C NMR spectra of the equilibrated ^{13}C enriched *tris*-La[(+)-L]$_2$ sample (CD_3CN, 7.2×10^{-3} M, rt). *, signals of the minor species observed at rt. +, signals of new species developing at low temperature. Rhombii, signals belonging to *tetra*- La[(+)-L]$_2$.

conversion *tris* to *tetra* by ^{13}C NMR spectroscopy, focusing only on the diagnostic signals from the marked carboxylic carbon atoms. The ^{13}C NMR spectra of pure, marked *tris*-LnL_2 complexes show two carboxylic resonances corresponding to the two sets **S** and **S′** while the spectra of *tetra*-Ln_4L_9 display three resonances corresponding to the sets **S″**, **S‴**, and $\mathbf{S^{IV}}$. Time dependent ^{13}C NMR experiments were performed at room temperature on CD_3CN samples with initial [*tris*-LnL_2]$_0$ concentration $\approx 7 \times 10^{-3}$ M. Considering the marked complex *tris*-La[(+)-L]$_2$, the two initial resonances corresponding to ligands of sets **S** (182.1 ppm) and **S′**(180.1 ppm) of *tris*-LnL_2 complex decrease in intensity with time. Three signals belonging to the sets **S″**(179.3), **S‴**(177.9), and $\mathbf{S^{IV}}$ (173.3) of the *tetra*-Ln_4L_9 species develop simultaneously (Figure 9a). The last spectrum, recorded 70 min after dissolving, corresponds to the equilibrated mixture with the signals of the *tetra*-Ln_4L_9 being the most intense. No peaks from *tris*-La[(+)-L]$_2$ are detectable, and it is possible to distinguish two additional resonances belonging to unassigned minor species developed during the conversion.

A comparison between the spectra excludes any correspondence between the signals of the unassigned species and the signal of the free ligand (reported in Figure 9b). This observation shows that the minor species contain also an organic part and excludes a conversion in which *all* the ligand builds up the tetranuclear structure, as expressed in the following chemical equation:

$$3[Ln_3L_6(OH)](ClO_4)_2 \rightleftarrows 2[Ln_4L_9(OH)](ClO_4)_2 + \{Ln^{3+} + OH^- + 2ClO_4^-\}$$

To gain insight into the nature of minor species, a series of temperature-dependent ^{13}C NMR spectra was registered on the equilibrated sample. The temperatures investigated ranged from 293 to 228 K. In the case of the La(III) species (Figure 10) the two most intense peaks from the minor species disappear upon lowering the temperature, with the simultaneous formation of a higher number of other less intense signals. This points to a substantial lability of the minor products in the mixture, easily interconverting upon external stimuli (temperature, in this case). It is noteworthy how the signals corresponding to *tetra*-Ln_4L_9 are instead unaffected by temperature changes, confirming the higher stability of this species.

The ^{13}C NMR spectrum registered at rt on a marked *tris*-Pr[(+)-L]$_2$ sample after conversion (Supporting Information, Figure 7) displays on the other hand not two but four minor signals. This can account for a different nature of the minor species in the two cases, in the conditions of the measurements (concentration and temperature), although neither NMR nor ES-MS investigations allowed their precise assignment.

The experiment run on isotopically labeled *tris*-Eu[(+)-L]$_2$ (Figure 11) showed a longer equilibration time (10 h) and a lower extent of conversion with a 1:1 *tris/tetra* ratio at equilibrium.

The evolution of *tris*-LnL_2 solutions in acetonitrile was monitored also by ^1H NMR spectroscopy affording accurate data on the equilibration time along the series Ln = La, Pr, Nd, Sm, and Eu. The assignement of the signals was made by comparison between the spectra of pure trinuclear compounds (two sets of ligands in 1:1 ratio, 13 signals for each set) and pure tetranuclear ones (three sets of ligands in 1:1:1 ratio, 13 signals for each set). These assignments were always confirmed via 2D NMR measurements (COSY and ROESY). We investigated the dependence of the conversion *tris* to *tetra* with respect to two parameters: (a) the initial concentration of trinuclear complex, [*tris*-LnL_2]$_0$; (b) the nature of the Ln(III) ion. A series of time dependent ^1H NMR spectra were collected starting from two different [*tris*-LnL_2]$_0$ in the selected range of concentrations 1.2×10^{-2}−5×10^{-3} M (excepted the case of *tris*-La[(+)-L]$_2$ complex, for which only one concentration is considered).

For all these samples, a progressive decrease is observed in time of the two initial sets of signals assigned to the trinuclear species. On the contrary, three new main sets corresponding to the tetranuclear structure develop simultaneously, together with signals belonging to the minor, unassigned species (Figure 12). Significant differences in the equilibration time are revealed along the series, with values progressively longer ranging from La(III) to Eu(III) complexes (Table 4).

The dependence of the conversion time on the size of the Ln(III) ions suggests that the crucial step of the process is the solvation of the *tris*-LnL_2 complex. The appearance of sharp *tetra*-Ln_4L_9 signals simultaneous to the decrease in

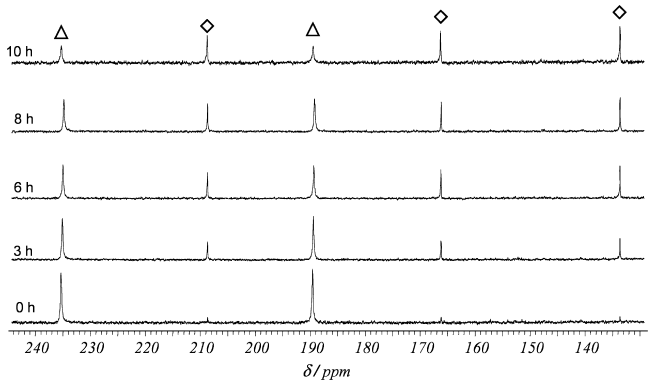

Figure 11. Evolution of the ^{13}C NMR spectrum upon conversion of ^{13}C marked *tris*-Eu[(+)-L]$_2$ in CD_3CN (7.5×10^{-3} M, rt). The times reported are intended after dissolution of the *tris*-LnL_2 complex. Triangles, signals relative to *tris*-Eu[(+)-L]$_2$ complex. Rhombii, signals relative to *tetra*-Eu_4[(+)-L]$_9$.

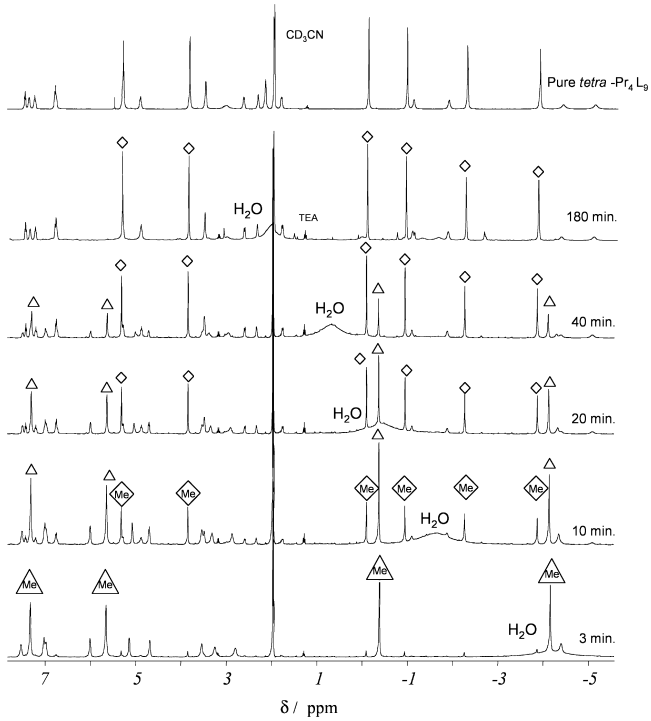

Figure 12. Time dependent ^1H NMR spectra collected on equilibrating *tris*-Pr[(+)-L]$_2$ solution in CD_3CN ($9.3 \cdot 10^{-3}$ M, rt). The methyl region is displayed. Triangles, *tris*-Pr[(+)-L]$_2$; rhombii, *tetra*-Pr_4[(+)-L]$_9$. The times reported are intended after dissolution of the solid sample of *tris*-Pr[(+)-L]$_2$. The spectrum of pure *tetra*-Pr_4[(+)-L]$_9$ in CD_3CN is reported for comparison.

Table 4. Equilibration Time and Final *tetra/tris* Ratio

compound	[*tris*-LnL_2]$_0$ (mol/L)	equilibration time	equilibration ratio *tetra:tris*
tris-La[(+)-L]$_2$	8.8×10^{-3}	(45 ± 5) min	>97:3
tris-Pr[(+)-L]$_2$	9.3×10^{-3}	(175 ± 10) min	>97:3
	4.6×10^{-3}	(110 ± 10) min	>97:3
tris-Nd[(-)-L]$_2$	1.1×10^{-2}	(300 ± 10) min	95:5
	5.2×10^{-3}	(175 ± 10) min	>97:3
tris-Sm[(+)-L]$_2$	9.2×10^{-3}	(415 ± 20) min	95:5
	5.0×10^{-3}	(330 ± 20) min	95:5
tris-Eu[(+)-L]$_2$	1.2×10^{-2}	16 h ± 30 min	55:45
	6.3×10^{-3}	9 h ± 30 min	80:20

intensity of *tris*-LnL_2 signals indicates that once part of the trimeric structure is decomposed, the fragments promptly reorganize with the nondecomposed *tris*-LnL_2 remaining in solution to afford the more stable $[Ln_4L_9(OH)]^{2+}$ species. A further hypothesis for explaining this behavior can be found by considering the coordination sphere of the metal centers. In the *tetra*-Ln_4L_9 structure the three coordinated water molecules which were present in the *tris*-LnL_2 compounds are substituted by three carboxylic oxygen atoms from the capping LnL_3 subunit. The stronger interaction of these coordinating water molecules to smaller Ln(III) ions (confirmed in the solid state by shorter Ln—OH_2 distances) prevents the coordination of competing CH_3CN molecules, thus conferring improved stability to the *tris*-LnL_2 structure.

Besides the longer equilibration times, another consequence of the stronger interaction of water with smaller Ln(III) ions is a lower extent of conversion, expressed by the presence of a large amount of *tris*-LnL_2 species in the equilibrated mixtures. This is the case of *tris*-Eu[(+)L]$_2$ solutions, which reach the equilibrium when a considerable part of *tris*-LnL_2 is still present (ratio *tetra/tris* almost 1:1 at 10^{-2} M). With larger Ln(III) ions (e.g., La and Pr) the *tris*-LnL_2 signals at equilibrium are at the limit of the integration, while with Ln = Nd and Sm about 5% of *tris*-LnL_2 is still detected.

Also, the initial concentration [*tris*-LnL_2]$_0$ has a significant effect on the rate of conversion and on the final *tetra* to *tris* ratio. Indeed for all the samples the equilibration times are shorter when more diluted solutions are used (Table 4). The dilution effect on the *tetra* to *tris* ratio at equilibrium is particularly evident in the case of the conversion of the *tris*-EuL_2 complex. The formation of *tetra*-Eu_4L_9 species is favored as compared with a more concentrated sample, and the *tetra* to *tris* ratio increases by up to 4 for [*tris*-EuL_2]$_0$ = 6×10^{-3} M.

The solvent-promoted removal of water from the first coordination sphere of Ln(III) ions in *tris*-LnL_2 compounds can be conveniently followed by ^1H NMR of paramagnetic *tris*-LnL_2 complexes in which the conversion is accompanied by a large shift of the water peak. The example of *tris*-Pr[(+)-L]$_2$ conversion is reported in Figure 12, focusing on the high field region of the spectra. In the first spectrum registered immediately after dissolution, it is possible to find the broad peak of water around −4.2 ppm, shifted to high field upon interaction with the paramagnetic Pr(III) centers. The signal corresponds to the water molecules in the first coordination sphere, in fast exchange with the free water in solution as confirmed by the line width of the peak. While the conversion *tris* to *tetra* and minor species is taking place, the peak of water undergoes a progressive low field shift until a final value of about 1.9−1.8 ppm, closer to the value of free water in CD_3CN (2.15 ppm). This accounts for a progressive weakening of the interaction between the paramagnetic metal center and water explained by the fact that in *tetra*-Ln_4L_9 complex the water molecules are no longer present in the first coordination sphere. Similar behavior is observed also in the spectra of Nd(III) and Eu(III) compounds.

If the displacement of water molecules from the first coordination sphere by acetonitrile molecules induces the conversion of *tris*-LnL_2 into *tetra*-Ln_4L_9 species, a reformation of *tris*-LnL_2 structure should be expected by adding an

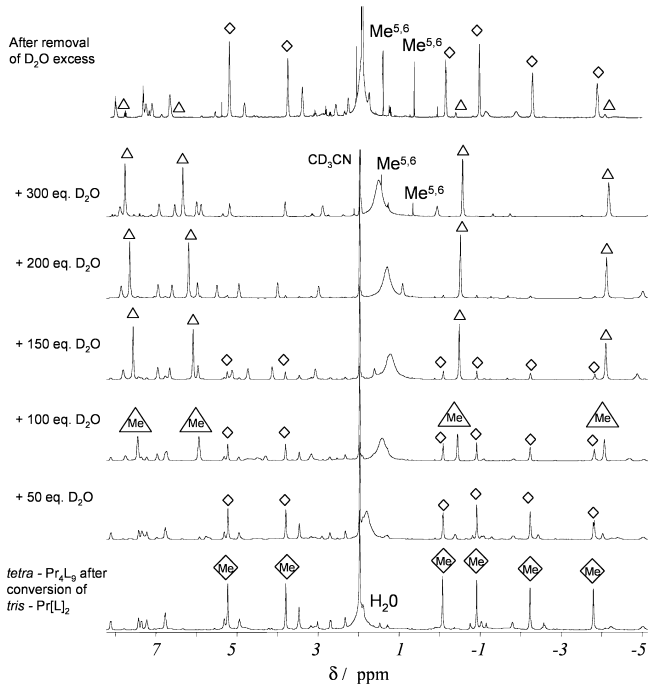

Figure 13. Water dependent evolution of ^1H NMR spectra of an equilibrated *tris*-$Pr[(+)\text{-}L]_2$ solution in CD_3CN ($[tris]_0 = 9.3 \times 10^{-3}$ M). The methyl region is displayed. Triangles, *tris*-$Pr[(+)\text{-}L]_2$; rhombii, *tetra*-$Pr_4[(+)\text{-}L]_9$. Methyl signals $Me^{5,6}$ from (-)-5,6-pinene bipyridine are revealed at the end of the conversion. The last spectrum was recorded after removal of the D_2O excess by molecular sieves.

excess of water to an equilibrated acetonitrile solution of *tris*-LnL_2. This *tetra* to *tris* reconversion was indeed observed when aliquots of D_2O were added to a freshly equilibrated solution of *tris*-$Pr[(+)\text{-}L]_2$ in acetonitrile, whose ^1H NMR spectrum displayed virtually no *tris*-LnL_2 species (Figure 13).

A large excess of D_2O was added (300 equiv per equiv of *tris*-LnL_2 complex) before the nearly complete disappearance of the peak of the *tetra*-Ln_4L_9 species (peaks at the limit of the detection) and the regeneration of the trinuclear species. The addition of water provoked as a side effect the reprotonation of the carboxylic moiety of a small amount of the coordinated ligand, which decarboxylates[61] and subsequently decomplexes. Weak signals $Me^{5,6}$ of the product of decarboxylation, the (-)-5,6-pinene bipyridine were individuated at the end of the conversion. The signals are weak (10% of *tris*-LnL_2 signals) but sharp, and their chemical shift corresponds to uncoordinated (-)-5,6-pinene bipyridine.

To prove the reversibility of the conversion process, molecular sieves were successively added to the solution above. The purpose was to reduce its water content and to verify if the pure trinuclear arrays will reform the initial mixture containing the *tetra*-Ln_4L_9 and minor species. Indeed the ^1H NMR spectra registered after the treatment with molecular sieves of all the complexes giving a measurable NMR spectrum (Ln(III) = La, Pr, Sm, Nd, Eu) show a drastic reduction of the peak of water. Concomitantly, the almost complete disappearance of *tris*-LnL_2 resonances and the rise of the three sets of *tetra*-Ln_4L_9 signals together with smaller peaks from minor species was observed (Figure 13).

(61) von Doering, W.; Pasternak, V. Z. *J. Am. Chem. Soc.* **1950**, *72*, 143.

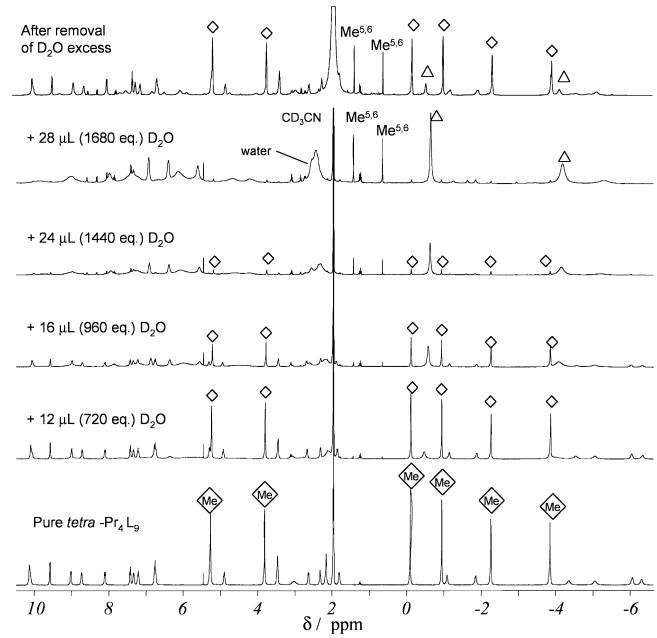

Figure 14. Evolution of ^1H NMR spectra of pure *tetra*-$Pr_4[(+)\text{-}L]_9$ (CD_3CN, $[tetra]_0 = 9.3 \times 10^{-3}$ M, rt) upon addition of aliquots of D_2O. Triangles, *tris*-$Pr[(+)\text{-}L]_2$; rhombii, *tetra*-$Pr_4[(+)\text{-}L]_9$.

In the above study, pure *tris*-LnL_2 compounds were dissolved in acetonitrile and their reversible transformation described. The pure *tetra*-Ln_4L_9 species proved to be stable in anhydrous acetonitrile, but an evolution of ^1H NMR spectra is observed after addition of water. The case of Pr(III) is given as an example in Figure 14.

Signals corresponding to *tetra*-Ln_4L_9 species are drastically reduced (about 5% of *tetra*-Ln_4L_9 still detected) and have been replaced by other signals, including signals attributed to *tris*-LnL_2 species. The process can be described by the general equation:

$$a'\,[Ln_4L_9(OH)](ClO_4)_2 \underset{CH_3CN}{\overset{CH_3CN + H_2O}{\rightleftharpoons}} b'\,[Ln_3L_6(OH))(H_2O)_3](ClO_4)_2 + \{c'\,Ln^{3+} + d'\,L^- + e'\,OH^- + f'\,ClO_4^-\}$$

where $c' = 3a' - 4b'$, $d' = 6a' - 9b'$, $e' = a' - b'$, and $f' = 2a' - 2b'$.

A broadening of the *tris*-LnL_2 signals is observed which is indicative of a fast exchange with other new formed species on the NMR time scale. This aspect combined with the increased complexity of the spectra observed in all the other Ln(III) compounds prevented more detailed, quantitative studies. Sharp signals corresponding to the (-)-5,6 pinene bipyridine are also detected, indicating that decarboxylation of part of the ligand took place upon reprotonation. The cycle of interconversion was completed, as in the preceding case, by absorbing the excess of water on molecular sieves. The ^1H NMR spectrum collected on the dried solution (Figure 14) accounted for a good but not quantitative reconversion of the mixture into *tetra*-Ln_4L_9 species (final ratio *tetra* to *tris* 7:3). The decarboxylated residue of the ligand, the (-)-5,6-pinene bipyridine is present as well (representing about the 10% of the total amount of the ligand).

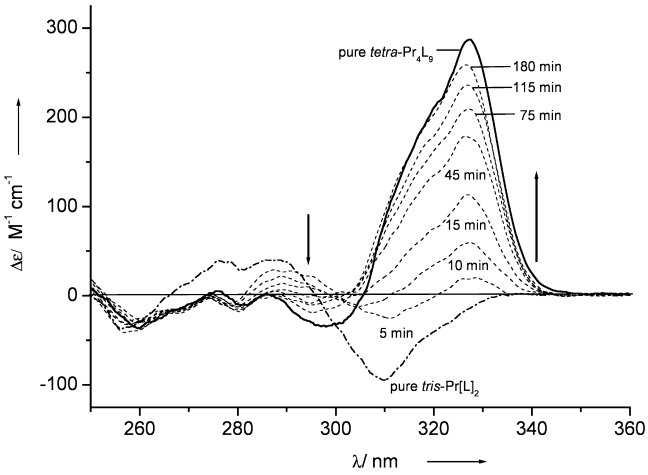

Figure 15. Time dependent evolution of the CD profile of *tris*-Pr[(+)-L]$_2$ in CH_3CN ($c = 1 \times 10^{-4}$ M, 20 °C). The spectra of pure *tris*-Pr[(+)-L]$_2$ (in CH_2Cl_2) and *tetra*-Pr$_4$[(+)-L]$_9$ (in CH_3CN) are reported.

Considering the high CD activity of the trinuclear and the tetranuclear species, the conversion *tris* to *tetra* in acetonitrile can be conveniently monitored also by CD spectroscopy. A series of time-dependent CD spectra was acquired on $\sim 10^{-4}$ M samples of *tris*-LnL$_2$ (Ln = La, Pr, Nd, Sm and Eu) in dry acetonitrile. The case of the *tris*-Pr[(+)-L]$_2$ complex is reported in Figure 15. It is generally observed that the component centered around 309 nm and exhibiting a negative $\Delta\varepsilon$ is progressively decreasing in absolute value of intensity while a lower energy band centered at 327 nm, characteristic of *tetra*-Ln$_4$L$_9$ species, is rising. The two smaller bands centered at 276 and 287 nm decrease as well during the conversion. The last spectrum of the conversion does not match perfectly the CD profile of a pure *tetra*-Pr$_4$L$_9$ sample, probably because of the presence of minor species formed upon conversion, which can contribute to the overall CD activity of the solution.

Switchable Racemates: the Role of Chiral Recognition. As illustrated with enantiopure complexes, also solutions of racemic *tris*-LnL$_2$ complexes in acetonitrile undergo a conversion leading to *tetra*-Ln$_4$L$_9$ species. The phenomenon was investigated by means of ES-MS and NMR spectroscopy. The chiral properties were monitored by CD and polarimetry. The flat CD spectrum recorded during the conversion time as well as the negligible optical rotatory power show that the racemic character of the mixture in all the cases is maintained upon conversion. A series of time-dependent ^{1}H NMR spectra on the racemate mixtures proved that the time of the conversion (Figure 16b) is not influenced by the enantiomeric purity. Nevertheless, there is a substantial difference in the composition of the final mixture, that is, the number and the amount of the "minor species" is clearly higher in the case of the racemates. It was unfortunately impossible to quantify unidentified minor species in the very complex spectra obtained. The ES-MS analysis on an equilibrated Pr(III) sample, allows to gain more information on the speciation in solution after conversion (Figure 16a). No peak from *tris*-LnL$_2$ species is detected. The signal of *tetra*-Ln$_4$L$_9$ molecular cation $[Pr_4L_9(OH)]^{2+}$ at $m/z = 1609$ is accompanied by the signal at $m/z = 727$ already detected

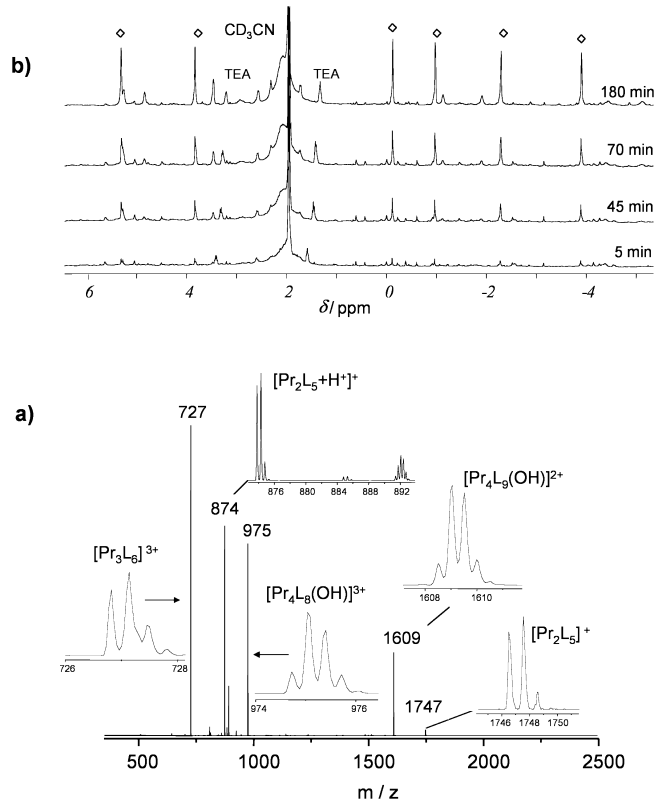

Figure 16. (a) ES-MS spectrum of equilibrated solutions of *tris*-Pr[(±)-L]$_2$ (CH_3CN, $c \approx 1 \times 10^{-4}$ M). (b) Time dependent ^{1}H NMR spectra collected on equilibrating *tris*-Pr[(±)-L]$_2$ solution in CD_3CN (8.0×10^{-3} M, rt). Methyl signals of *tetra*-Pr$_4$[(±)-L]$_9$ species indicated with rhombii.

in the spectrum of the enantiomerically pure *tris*-Pr[(+)-L]$_2$ after conversion (vide supra). The isotopic pattern accounts for the triple charged cation $[Pr_3L_6]^{3+}$. Two related peaks are moreover observed at $m/z = 1747$ ($[Pr_2L_5]^+$) and at 874, protonated adduct ($[Pr_2L_5+H^+]^{2+}$) probably formed during the ionization process. The peak at $m/z = 975$ corresponds instead to the triple charged fragment $[Pr_4L_8(OH)]^{3+}$. In conclusion, a comparison with the ES-MS spectrum of an equilibrated solution of enantiopure *tris*-Pr[(+)-L]$_2$ points to a higher complexity of the racemic mixture, confirming the presence of additional minor species, as already revealed by NMR.

The evolution of acetonitrile solutions of *tris*-Eu[(±)-L]$_2$ followed by means of ^{1}H NMR accounted, as in the case of the enantiopure sample, for an incomplete *tris* to *tetra* conversion (Supporting Information, Figure 8). However, here the predominant signals do not correspond to *tris*-LnL$_2$ or *tetra*-Ln$_4$L$_9$ compounds but to unassigned species detected in significant extent already in the first spectra. After the conversion, the peaks from *tetra*-Ln$_4$L$_9$ species are among the most intense, but signals from *tris*-LnL$_2$ are still detected. The ES-MS analysis performed on an equilibrated sample diluted to 10^{-4} M indicated that this species could correspond to the molecular cation $[Eu_2L_5]^+$ detected at $m/z = 1769$ as the major signal. This would be consistent with the corresponding signal observed for the equilibrated *tris*-Pr[(±)-L]$_2$ solution. In the present spectrum is also detected the peak of $[Eu_nL_{2n}]^{n+}$ species ($m/z = 738$), already observed in the

mass spectrum of the converted homochiral *tris*-Eu[(+)-L]$_2$ complex.

A comparison with the spectrum of the equilibrated solution of all enantiopure *tris*-LnL$_2$ complexes, which appear drastically more simple, confirms that the conversion *tris* to *tetra* and minor species is perturbed by the initial presence of two enantiomeric complexes in solution. In fact, the reorganization of the fragments upon dissolution of *racemates* in acetonitrile depends strongly on the effectiveness of the initial chiral recognition step. The results obtained have shown clearly that the chiral recognition is only partial and affects significantly the final outcome of the self-assembly process.

Conclusions

We have demonstrated that the chiral ligand HL, a carboxylic derivative of the 5,6-pinene bipyridine, is a versatile building block for the Ln(III) ions able to self-assemble diastereoselectively two enantiopure helical architectures via two distinct solvent-controlled reaction pathways. The trinuclear class of compounds with the formula [Ln$_3$L$_6$(μ_3-OH)(H$_2$O)$_3$](ClO$_4$)$_2$ (Ln(III) = La, Pr, Nd, Sm, Eu, Gd, Tb, Dy, Ho, Er) obtained in methanol were previously described. If the solvent used is acetonitrile then a tetranuclear class of compounds with the formula [Ln$_4$L$_9$(μ_3-OH)](ClO$_4$)$_2$ (Ln(III) = La, Pr, Nd, Sm, Eu, Gd, Tb) is quantitatively obtained. Structurally there is a close relationship between these architectures: three metal ions forming the triangular base are surrounded by two sets of coordinatively distinct ligands building up two helical domains with opposite configurations. In the case of tetranuclear species a new helical unit LnL$_3$ completes the assembly giving rise to a pyramidal trigonal structure containing three helical domains. In the case of smaller Ln(III) ions (Dy, Ho, Er) the trinuclear base is probably too small to accommodate the capping LnL$_3$ unit. Here complex mixtures of oligonuclear species are obtained. Detailed solution studies (ES-MS, NMR, CD) proved that the structures obtained in solid state are maintained in CH$_2$Cl$_2$ and anhydrous acetonitrile. The compounds possess a strong CD activity and interesting emission properties in visible (Eu(III) and Tb(III) complexes) and IR (Nd(III) complex). When a racemic mixture of the ligand is used in the self-assembly, the system does not show significant chiral recognition capabilities. A complicated mixture is obtained—a behavior which can be rationalized by the complexity introduced by the high number of components (9 ligands (+), 9 ligands (−), and 8 metal ions) which have to assemble to give a perfect racemate.

We have demonstrated as well that the trinuclear and tetranuclear compounds can be reversibly interconverted. The dissolution of pure trinuclear species in acetonitrile lead to their total or partial disassembly and the formation of tetranuclear structures accompanied by other minor species. If a certain amount of water is added then the trinuclear species are reformed quantitatively. Detailed investigations (NMR, CD, ES-MS) of these interconversions revealed their dependence on parameters like concentration, water content, lanthanide ionic radius, and enantiomeric purity of the ligand. The presence of water clearly proved to stabilize the trinuclear species to the detriment of the tetranuclear ones. Using the molecular sieves, the amount of water is reduced and the tetranuclear species are reformed. The number of these reversible cycles is, however, limited by the partial decarboxylation[61] of the ligand in the presence of water.

Acknowledgment. This work was supported by the Swiss National Science Foundation (Grant 200020−105320).

Supporting Information Available: Tables with the attribution of the three sets of ^{1}H NMR signals and ROESY *inter*-ligand contacts revealed for *tetra*-Ln$_4$L$_9$ complexes; ES-MS and IR spectra of pure *tetra*-Ln$_4$L$_9$ structures; ES-MS, ^{1}H NMR, and ^{13}C NMR spectra monitoring the conversion process *tris*-LnL$_2$ to *tetra*-Ln$_4$L$_9$; the cif file of the structure [Nd$_4${(+)-L}$_9$(μ_3-OH)](ClO$_4$)$_2$). This material is available free of charge via the Internet at http://pubs.acs.org.

IC7021006